STATUS REPORTS

To The

PAPER PHYSICS

PROJECT ADVISORY COMMITTEE

March 21 - 22, 1995

INSTITUTE OF PAPER SCIENCE AND TECHNOLOGY

Atlanta, Georgia

ANNUAL RESEARCH REVIEW

PAPER PHYSICS

March 21 - 22, 1995

February 13, 1995

TO: MEMBERS OF THE PAPER PHYSICS PROJECT ADVISORY COMMITTEE

Attached for your review are Status Reports for projects to be reviewed and discussed at the Paper Physics PAC meeting scheduled for March 21-22, 1995, in Atlanta. A meeting agenda can be found inside the booklet.

Please note that the meeting is being held at the Institute of Paper Science and Technology.

We look forward to seeing you at this time.

Sincerely,

David I. Orloff, Ph.D.
Professor of Engineering & Director
Engineering and Paper Materials Division

DIO/map

Attachment

Institute of Paper Science and Technology, Inc.

500 10th Street, N.W.
Atlanta, GA 30318-5794

Telephone 404-853-9500
FAX # 404-853-9510

PAPER PHYSICS
PROJECT ADVISORY COMMITTEE

IPST Laision: David Orloff (404) 853-1872, FAX (404) 853-9510

Dr. Thomas E. Altman *(1997) (Vice Chairman)
Research Scientist
Union Camp Corporation
P. O. Box 3301
Princeton, NJ 08543-3301
(609) 844-7428
(609) 844-7323 FAX

Dr. George L. Batten, Jr. *(1997)
Manager of Research & Development
Georgia-Pacific Corporation
2883 Miller Road
Decatur, GA 30035-4036
(404) 593-6837
(404) 593-6801 FAX

Dr. Keith A. Bennett *(1994)
Senior Research Scientist
Weyerhaeuser Company
WTC 2B22
Tacoma, WA 98477-0001
(206) 924-6714
(206) 924-4207 FAX

Dr. William Boyd *(1997)
Research Physicist
Buckeye Cellulose Corporation
1001 Tilman Street
P. O. Box 8407
Memphis, TN 38108
(901) 320-8100
(901) 320-8394 FAX

Dr. Kraig M. Brigham *(1996)
Manager, Product Development
P. H. Glatfelter Co.
Ecusta Division - P. O. Box 200
32 Red Fox Drive
Pisgah Forest, NC 28768-6000
(704) 877-2313
(704) 877-2385 FAX

Dr. John Goss *(1997)
Director, Sensor Products
Measurex Corporation
One Results Way
Cupertino, CA 95014
(408) 255-1500

Mr. Thomas G. Gulya *(1996)
Manager - Research & Development
Asten Group, Inc.
Asten Forming Fabrics, Inc.
P. O. Box 8005
Appleton, WI 54913-8005
(414) 734-2607
(414) 734-4229 FAX

Dr. Thomas C. Kisla *(1996)
Manager, Energy Source
Planning & Development
Stone Container Corporation
1979 Lakeside Parkway, Ste. 300
Atlanta, GA 30084-5847
(404) 621-6714
(404) 621-6733 FAX

Mr. Håkan Markström *(1996)
Research Manager
Lorentzen & Wettre
Box 4, 164 93 KISTA
KISTA , Stockholm, Sweden
011-46-8 752 01 60
011-46-8 752 93 00 FAX

Dr. Leslie L. Martin *(1995) (Chairman)
Manager Papermaking R & D
Potlatch Corporation
Fiber R & D - P. O. Box 503
East End Ave. E
Cloquet, MN 55720-0503
(218) 879-2387
(218) 879-2375 FAX

Mr. William W. Maslanka *(1997)
Research Associate
Hercules Incorporated
Research Center
500 Hercules Road
Wilmington, DE 19808-1599
(302) 995-3115
(302) 995-4565 FAX

Dr. William J. McNown *(1996)
Research Engineer
Westvaco Corporation
Research Center - Mill Road
Covington, VA 24426-0950
(703) 969-2452
(703) 969-2448 FAX

* The dates in ( ) indicate the final year of the appointment.

Revised 10/25/94:lkh

Paper Physics PAC (cont.)

Dr. Robert J. Niebauer *(1997)
Project Manager, R & D
Crane & Co., Inc.
30 South Street
Dalton, MA 01226-1751
(413) 684-2600
(413) 684-0726 FAX

Mr. Dirk E. Swinehart *(1995)
Fellow, Paper Physics
Mead Central Research
The Mead Corporation
Eighth & Hickory Streets
Chillicothe, OH 45601-5700
(614) 772-3570
(614) 772-3595 FAX

Mr. Dan H. Sze *(1997)
Manager, Paper Technology
Beloit Corporation
Rockton Research Center
1165 Prairie Hill Road
Rockton, IL 61072-1595
(608) 364-8525
(608) 364-8600 FAX

Mr. William A. Wiberg *(1996)
Technical Manager - Biron Division
Consolidated Papers, Inc.
Corporate Offices
P. O. Box 8050
Wisconsin Rapids, WI 54495-8050
(715) 422-3111
(715) 422-3469 FAX

* The dates in ( ) indicate the final year of the appointment.

Revised 10/25/94:lkh

PAPER PHYSICS
PROJECT ADVISORY COMMITTEE MEETING

March 21 - 22, 1995
Institute of Paper Science and Technology
Atlanta, Georgia

AGENDA

Paper Physics Program Review (APR)

March 21, 1995

1:00 p.m. - 1:15 p.m.	Opening Remarks and Anti Trust Statement	Les Martin
1:15 p.m. - 2:15 p.m.	Project F007/3942 On-Line Measurement of Paper Properties	Mac Hall
2:15 p.m. - 3:00 p.m.	Project E00102 Dimensional Stability	Doug Coffin
3:00 p.m. - 3:15 p.m.	Break	
3:15 p.m. - 4:45 p.m.	Project F008-03/3767-03 Fundamentals of Acoustic Radiation Pressure	Pierre Brodeur

March 22, 1995

8:00 a.m. - 12:00 p.m.	Paper Physics Committee Discussions	David Orloff

TABLE OF CONTENTS

FUNDAMENTALS OF ACOUSTIC RADIATION PRESSURE

STATUS REPORT

FOR

PROJECT F008-03/3767-03

Pierre Brodeur
Joe Gehardstein

March 21 - 22, 1995

Institute of Paper Science and Technology
500 10th Street, N.W.
Atlanta, Georgia 30318

TECHNICAL PROGRAM REVIEW

Project Title:	FUNDAMENTALS OF ACOUSTIC RADIATION PRESSURE
Project Code:	FARPE
Project Number:	3767-3/F008-03
Division:	Engineering and Paper Materials Division
Project Staff:	Pierre Brodeur, Joe Gehardstein
Project Budget:	$84,688

OBJECTIVES

- Investigate fundamentals of acoustic radiation pressure (ARP) effects on fiber suspensions;
- Investigate mechanisms of acoustic fiber agglomeration and reorientation;
- Demonstrate the concept of acoustic wet fiber flexibility/compactibility;
- Demonstrate the concept of acoustic fiber separation/fractionation;
- Explore other process-related applications of acoustic radiation pressure, acoustic cavitation, and acoustic streaming;
- Determine the economic viability of acoustically-based industrial processes.

SUMMARY

During the past year, we continued the development of an experimental research program to study various effects of acoustic radiation pressure on water suspended fibers. The program was sufficiently mature to be structured into several interrelated sub projects: acoustic cell characterization, acoustic wet fiber flexibility, acoustic compactibility of a fiber mat, acoustic fiber separation/fractionation, and acoustic fiber reorientation.

Regarding the characterization of the acoustic cell, a relationship was obtained between the electrical power delivered to the transducer and the acoustic power. Also, two independent methods were tested to determine the acoustic radiation force. Results were used to validate the procedure to measure the acoustic power.

In the area of wet fiber flexibility, observations of cantilever-mounted fibers subjected to a distributed acoustic load indicated that the fibers did not bend as expected. Instead, some fibers could not sustain the acoustic load and were sectioned. This "refining" effect was attributed to an apparent increase of fiber stiffness due to the 150 kHz oscillating load. This is a consequence of the viscoelasticity of wood pulp fibers.

Unexpected results about fiber flexibility triggered the development of a modified setup to investigate the compactibility of a wet fiber mat due to a traveling wave field. A series of preliminary experiments were performed using softwood fibers beaten to various levels using a Valley beater. Results were obtained at 0.5% and 1% consistency. A relationship was found between the beating time and the differential cross-sectional area of the fiber mat as obtained with and without the acoustic load. Measurements did not appear to be sensitive to consistency.

We decided to go ahead with the development of a prototype acoustic fiber separation/fractionation system. A traveling wave field separation configuration was implemented. An adjustable mechanical divider with two output streams was installed above the acoustic cell to collect coarser and slender fibers. Preliminary trials using softwood fibers at 0.5% consistency indicated that the system was capable of producing high and low consistency fractions.

Finally, the laser-based optical monitoring system to study acoustic fiber agglomeration and reorientation was fully implemented.

VALUE TO THE INDUSTRY

The long-term streamline of project F008 is to provide the scientific and technical basis for the development of novel ultrasonic instruments and/or processing technologies that would benefit the pulp and paper industry.

Possible outcomes of the current work about acoustic fiber flexibility/compactibility would be the development of on-line instrumentation for fiber compactibility and refining monitoring and the development of acoustic refining technologies.

Research about the use of an acoustic field to separate and/or fractionate wood pulp fibers might lead to the development of on-line adaptable industrial fiber separation processes. As acoustic fractionators might be capable of processing continuously varying furnishes or be reprogrammed to meet different separation requirements, they could considerably increase the return on capital investment. As an example, while pressure-screen fractionators are dedicated mechanical systems, acoustically-based fractionators, which would be free of moving parts, might provide far more flexibility by allowing electrically-driven parameters to control separation.

Acoustic forming, which would be an evolved concept of acoustic separation, might provide the basis for furnish/product adaptable forming processes and diversify the use of a paper machine. Here again, the return on capital investment might be very high. One can envision among other concepts

acoustic positioning of short and long fibers in the sheet, three-dimensional fiber alignment, and preforming of one or more fiber layers.

The expertise gained during the project could also be used to develop other processes using high-power ultrasounds: clarification; deinking; solid waste agglomeration; turbulence; flocculation; enhanced combustion in recovery boilers.

A very stimulating review of industrial applications of sound was recently published in the January 95 issue of Delta Sky Magazine.[1]

PROJECT HISTORY

Project F008 was initiated in July 1992. Design, construction, and preliminary testing of a small-scale acoustic cell to study acoustic radiation pressure effects on water suspended fibers were completed during FY 92-93. The construction of a basic experimental setup was undertaken during FY 93-94. Qualitative observations of fiber agglomeration at various flow rates and consistency levels (up to 1%) were obtained during the second year.

ACCOMPLISHMENTS

The following activities were accomplished since January 1994:

- Acoustic Cell Characterization (Mr. Troy Runge, M.S. Student; Mr. Joe Gehardstein, Assistant Engineer)

  The relationship between the electrical power delivered to the transducer and the useful power in the acoustic cell was determined. Also, two independent methods were successfully tested to

evaluate the acoustic force acting on cylindrical particles. Results were used to validate the procedure to measure the acoustic power.

- Acoustic Wet Fiber Flexibility (Mr. Troy Runge, M.S. Student)

  A series of experiments were performed to demonstrate the concept of wet fiber flexibility using single-fibers mounted as cantilever beams. Observations indicated that the fibers did not generally deflect as expected even though the acoustic power was more than adequate. Instead, fibers were broken (refined) by the distributed acoustic load. This phenomenon was attributed to the viscoelastic properties of wood pulp fibers. In the presence of a high frequency, oscillating load fibers cannot relax. As a consequence, there is a buildup of stiffness and an apparent increase of brittleness.

- Acoustic Wet Fiber Compressibility (Mr. Troy Runge, M.S. Student)

  Unexpected results about fiber flexibility led to the rapid development of a modified setup to study the compactibility of a fiber mat in the acoustic cell. An optimized traveling wave field was used. Results obtained using Kraft softwood fibers subjected to five different beating levels provided enough evidence to support a simple relationship between acoustic compactibility and beating level.

- Acoustic Fiber Separation/Fractionation (Mr. Keit Ma, M.S. Student; Mr. Joe Gehardstein, Assistant Engineer)

  A mechanical divider with two output streams was installed on one end of the acoustic cell to demonstrate the concept of acoustic fiber separation/fractionation. A traveling wave field

separation configuration was implemented. The system is operated in a batch mode. Preliminary observations showed that high and low consistency fractions are easily obtained.

- Acoustic Fiber Agglomeration and Reorientation (Mr. Joe Gehardstein, Assistant Engineer)

  The development of a laser-based optical system to monitor the motion of fibers in the acoustic field was completed. Various polarization schemes are now investigated to detect fiber reorientation independently from fiber agglomeration.

- Ultrasonic Deinking (Mr. Eric Watkins, Ph.D. Student - A390 Problem)

  An exploratory study of a novel ultrasonic concept to separate ink particles from fibers was conducted.

- Research Proposal Titled: "Acoustic Fiber Fractionation"

  In response to a Notice of Program Interest from the Department of Energy, a proposal was completed in October 1993 to demonstrate the concept of acoustic fiber fractionation from laboratory- to pilot-scale level. Results from the competition are not available yet.

EXPERIMENTAL SETUP

A schematic of the basic experimental setup to study water-suspended fibers interacting with an acoustic wave field is depicted in Figure 1. One distinguishes on the right side an in-line acoustic cell mounted vertically to decouple gravitational and acoustic fields. A peristaltic pump is used to precisely control the flow rate in the continuous flow loop. Zero-flow and laminar flow conditions are possible. The suspending medium can be either tap or degassed water. A constant temperature circulator is available to perform experiments at different temperature levels. Fiber consistency can be up to 1%.

A schematic of the acoustic cell is shown in Figure 2. It consists of four identical and removable modular wall sections. These sections are used to support either a transducer, a reflector plate, an absorber plate, or a viewing port (glass window). The nominal length and width of these components are 100 mm and 20 mm, respectively. Figure 2 illustrates the case of a one-dimensional unbalanced resonator configuration (transducer-reflector assembly).

The narrow-band, single-element transducer was designed to resonate at 150 kHz. Its rectangular cross section ensures that every fiber penetrating the acoustic field is submitted to the same acoustic dwell length. Considering an approximate sound velocity in water of 1500 m/s at room temperature, the acoustic wavelength is 10 mm. When a standing wave field is prescribed (transducer-reflector assembly), four agglomeration planes are produced. When a traveling wave field is used (transducer-absorber assembly), fibers are pushed against the absorber.

A computer-controlled function generator and a broadband power amplifier are used to drive the transducer. A rod-mounted, calibrated, 5 mm diameter, sub-MHz P(VDF-TrFE) hydrophone is used

to evaluate field uniformity, pressure, and power in the acoustic cell. Acoustic wavelength and power are stabilized against temperature variations by using a thermocouple mounted on the transducer and a computer-controlled temperature compensation system. A CCD camera and an imaging system are used to record ARP effects. An argon-ion, laser-based system is also used to study agglomeration and reorientation effects. The optical system is further described below.

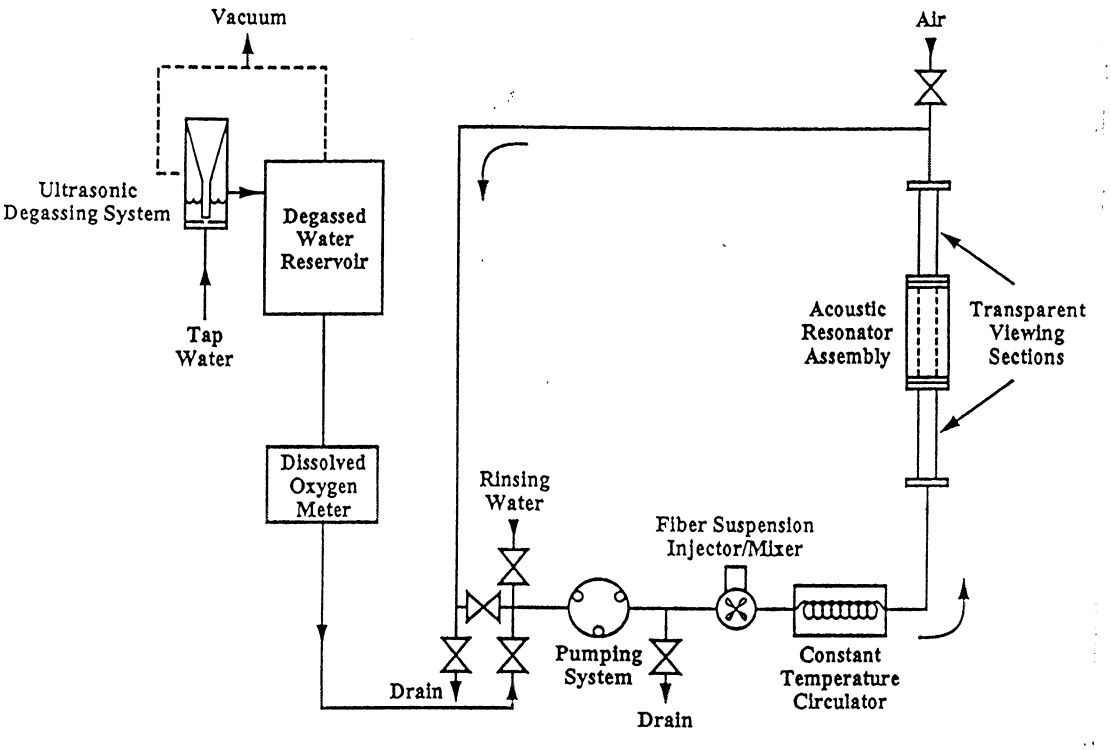

Figure 1. Schematic of the basic experimental setup to study ARP effects.

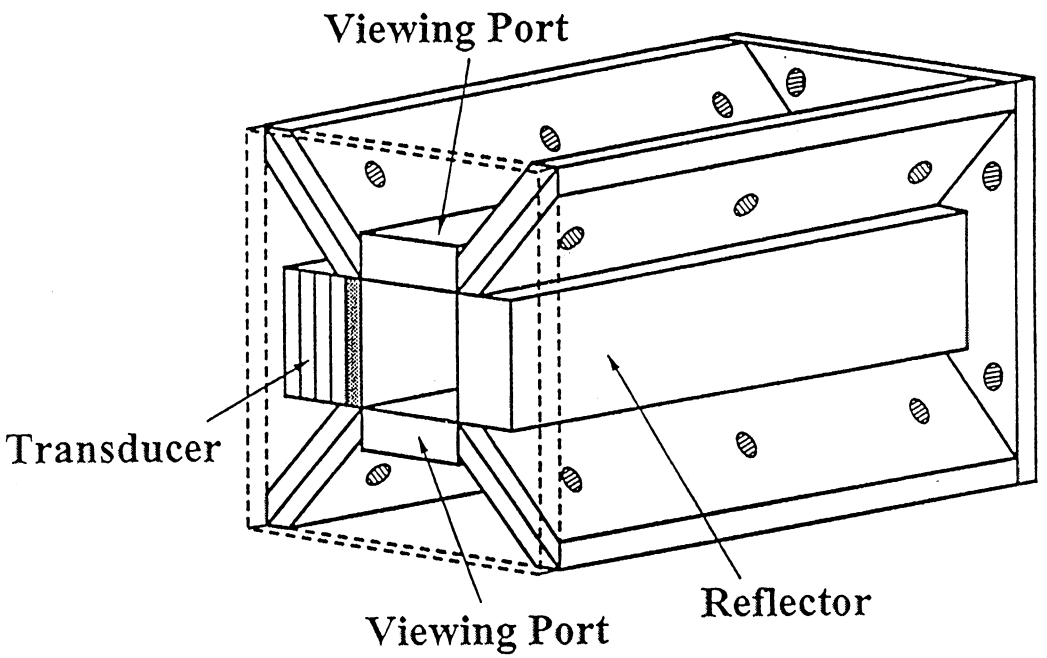

Figure 2. Schematic of the acoustic cell. Components dimensions are as follows: length, 100 mm; width, 20 mm.

ACOUSTIC CELL CHARACTERIZATION

We invested a fair amount of time during the past year to establish a relationship between the electrical power delivered to the transducer and the acoustic power. We were also able to develop two independent methods to determine the acoustic radiation force acting on the fibers (standing wave field configuration). Since there was good agreement between the two methods, we were able to validate the accuracy of acoustic power measurements.

The calibrated hydrophone was used to determine the acoustic power. It was mounted to a three-dimensional translation system located above the acoustic cell. An oscilloscope was used to determine the AC signal at 150 kHz. Figure 3 shows a mapping of the RMS acoustic power as

obtained every 0.5 mm from the transducer's position to the reflector's position. The RMS electrical power was set to 51.4 W. It was not possible to get data near the reflector due to physical constraints. The dashed line represents the predicted acoustic power for an ideal resonator; it is calibrated to fit experimental data. Results show that the resonator is far from ideal (perfect plane standing wave field everywhere in the cavity). Contrary to expectation, the acoustic power is not constant from node to node. Possible explanations are transducer's edge effects due to the relatively small dimensions of the acoustic cell, sound scattering in the cavity, inhomogeneity of the transducer's surface.

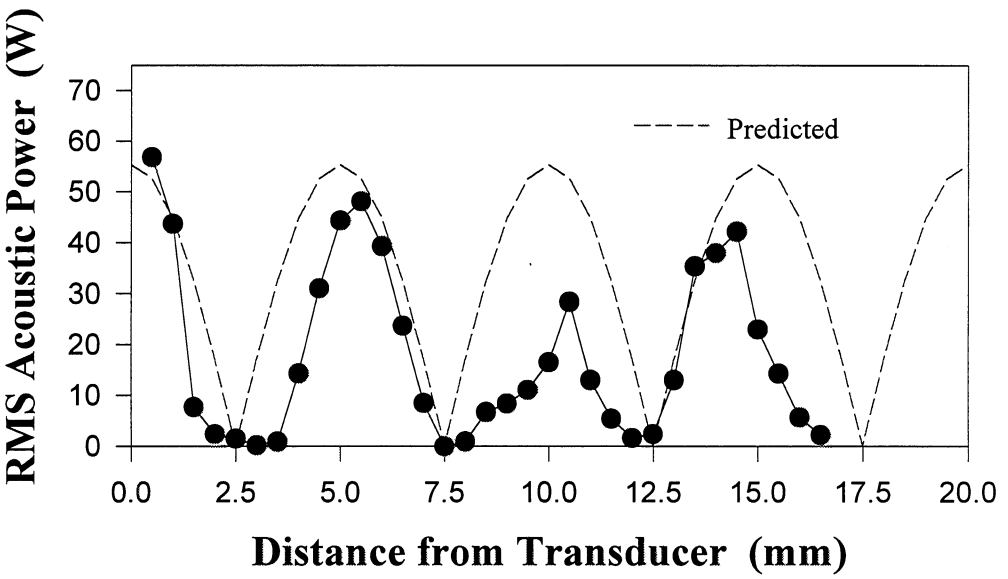

Figure 3. Plot of the RMS acoustic power as a function of distance from the transducer. The dashed line represents the power for an ideal resonator after calibration to fit experimental data.

It is interesting to note that the maximum measured acoustic power is approximately 50 W_{RMS} for a 51.4 W_{RMS} electrical power. This would tend to support that the electrical and mechanical coupling efficiencies in the system are near ideal conditions. But this is not the case as we know that the impedance matching conditions between the power amplifier and the transducer are not optimized. Instead, the reason is that there is a buildup of power due to resonance.

Two independent methods were tested to evaluate the acoustic force acting on water suspended cylindrical particles. In the first method we used the hydrophone to determine the acoustic pressure (proportional to acoustic power) and the theoretical equation[2] to predict the acoustic force acting on a rigid cylinder in a standing wave field. This equation is a function of the acoustic pressure, p_0.

$$F_{sw} = f(\beta)\frac{\pi a^2}{2}\overline{E}\,k\,\sin[2kh] \tag{1}$$

where $f(\beta) = \left[\frac{2(1-\beta)}{(1+\beta)} + 1\right]$ is the inertia factor; $\beta = \frac{\rho_0}{\rho_1}$ is the ratio of the suspending medium density to cylinder density; $k = \frac{2\pi}{\lambda}$ where λ is the acoustic wavelength; $\overline{E} = \frac{1}{2\rho_0}\left(\frac{p_0}{c}\right)^2$ is the mean energy density; p_0 is the static pressure (RMS acoustic pressure); c is the sound velocity; h is the cylinder center of mass position with respect to a nodal velocity plane.

The second method was developed during the course of single-fiber wet flexibility experiments (see below). The procedure for fiber flexibility involves mounting fibers on the tip of a metal rod which can be positioned anywhere inside the acoustic cell. We found that the metal rod deflected upon the onset of the acoustic field. Taking advantage of this effect, we were able to use the imaging system

to gather quantitative measurements of the distributed acoustic load. This was accomplished by comparing images obtained without and with the acoustic field. A schematic of the deflection arrangement is shown in Figure 4. The distance b corresponds to the section of the rod located within the acoustic cell.

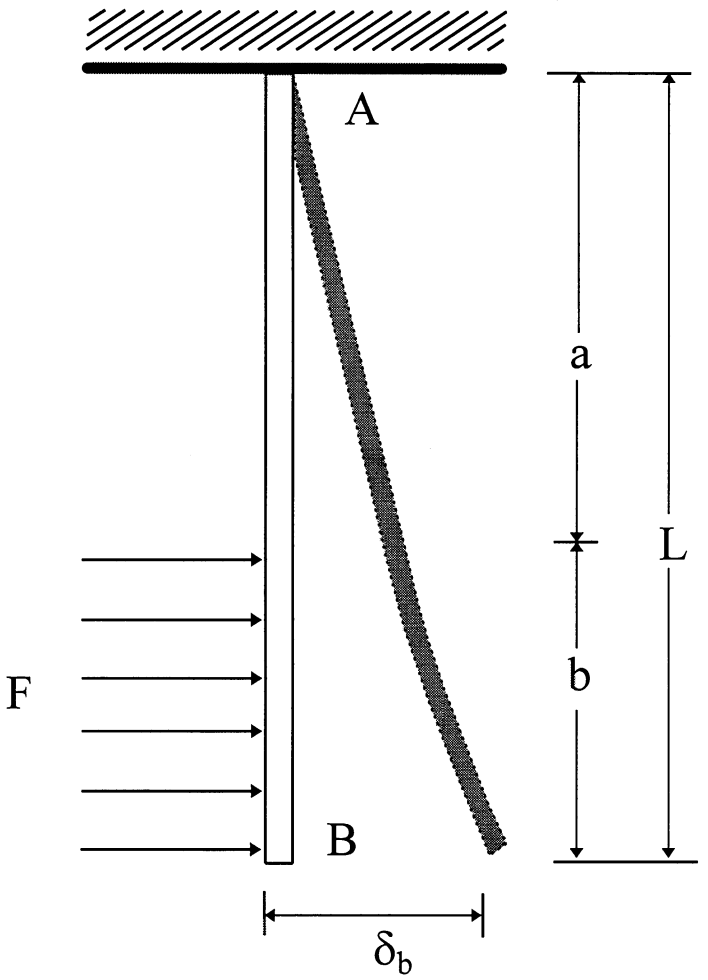

Figure 4. Deflection of a cantilever beam due to a localized distributed acoustic load.

For the case of a cantilever beam subjected to a distributed force, the tabulated equation relating the force and maximum deflection is as follows:

$$F = \frac{24EI\delta_B}{\left(3L^4 - 4a^3L + a^4\right)} \tag{2}$$

where δ_B is the maximum deflection.

Figure 5 shows a typical image analysis result. Also shown in this figure are rod parameters and the measured acoustic force. The modulus of elasticity was found from experiments using the rod as a cantilever beam. The rod was mounted horizontally, and a small weight was attached to its free end. The measured value, i.e., 194 GPa, agrees with tabulated data for mild steel.

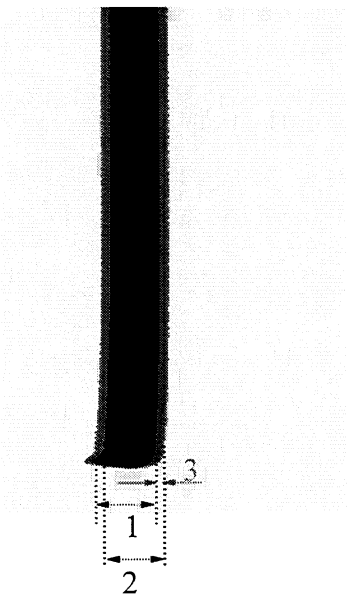

Rod is mild grade steel
E= 194 GPa
d = 0.50 mm
L = 145 mm
b = 59 mm
δ_B = 0.0737 mm
El. Power = 33.8 W_{RMS}
Force = 6.33 x 10^{-5} N
1 is the initial position
2 is position with acoustic field on
3 is the deflection (δ_b)

Figure 5. Typical image analysis result of the metal rod subjected to a distributed acoustic load.

Force measurements using the hydrophone method (electrical) and the rod deflection method (mechanical) are shown in Figure 6 as a function of the electrical power. Measurements were obtained at constant rod position with respect to the transducer. Since the two methods are based on very different measuring principles, the agreement is well above expectations. If one plots rod deflection force measurements as a function of hydrophone force measurements for various rod positions and power levels, a linear relationship is obtained. This is shown in Figure 7. Since the correlation is very good ($R^2 = 0.94$), we can validate the hydrophone method to determine the acoustic power. Moreover, we have an experimental confirmation of Equation 1. The 17% offset between mechanical and electrical measurements can be attributed to several factors: pressure measurements are affected by the physical size of the hydrophone; hydrophone and rod have different geometries, hydrophone calibration may be off.

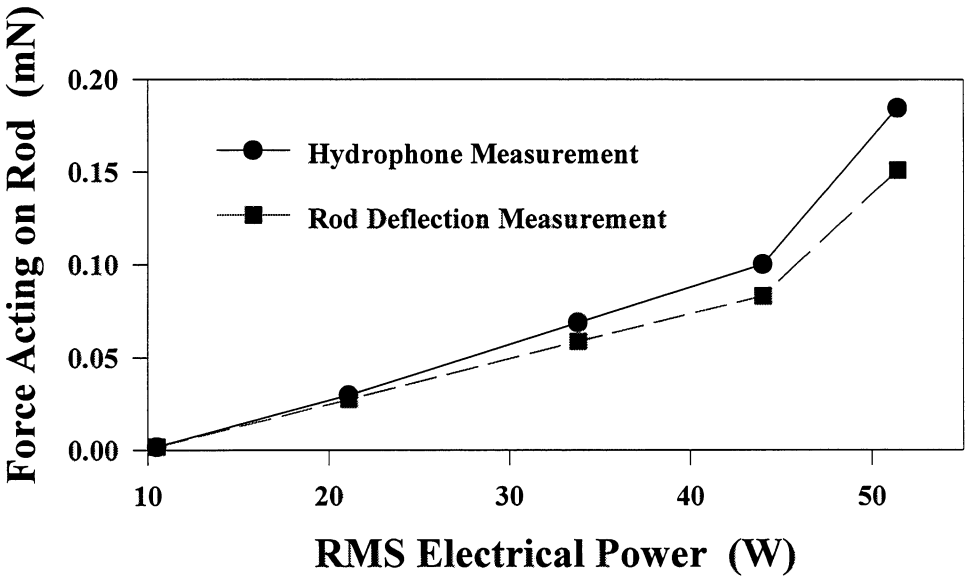

Figure 6. Force acting on the rod as a function of the RMS electrical power. Measurements were obtained at constant rod position with respect to the transducer.

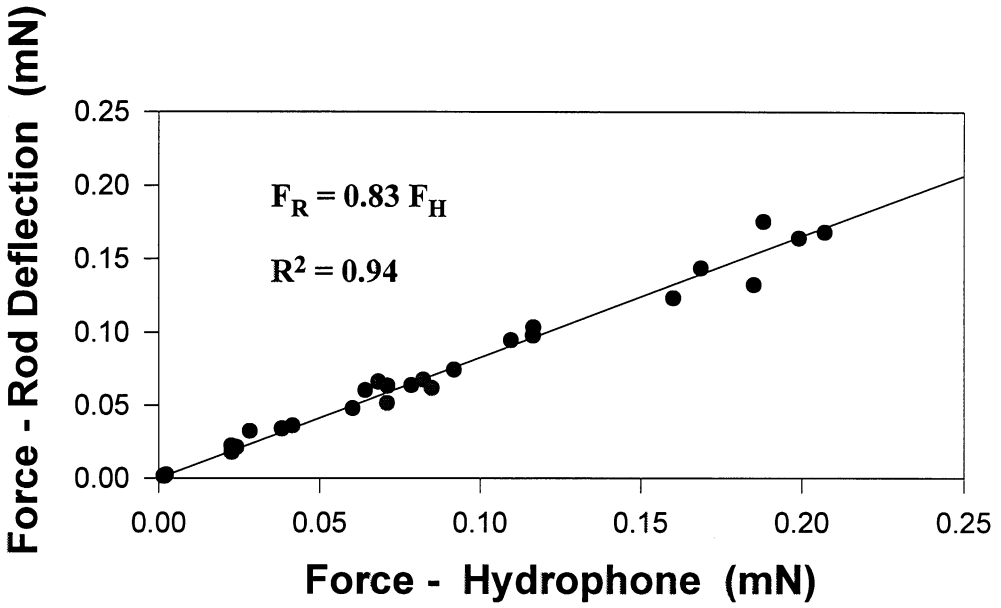

Figure 7. Plot of the force-rod deflection vs. force-hydrophone. Measurements were obtained for various rod positions and power levels.

ACOUSTIC WET FIBER FLEXIBILITY

One of the objectives of Project F008 concerns the demonstration of a noncontact acoustic method to determine the flexibility of wet fibers. It was first decided to investigate the flexibility of cantilever-mounted single fibers subjected to a distributed acoustic load in a standing wave field. A schematic of the testing method is shown in Figure 8.

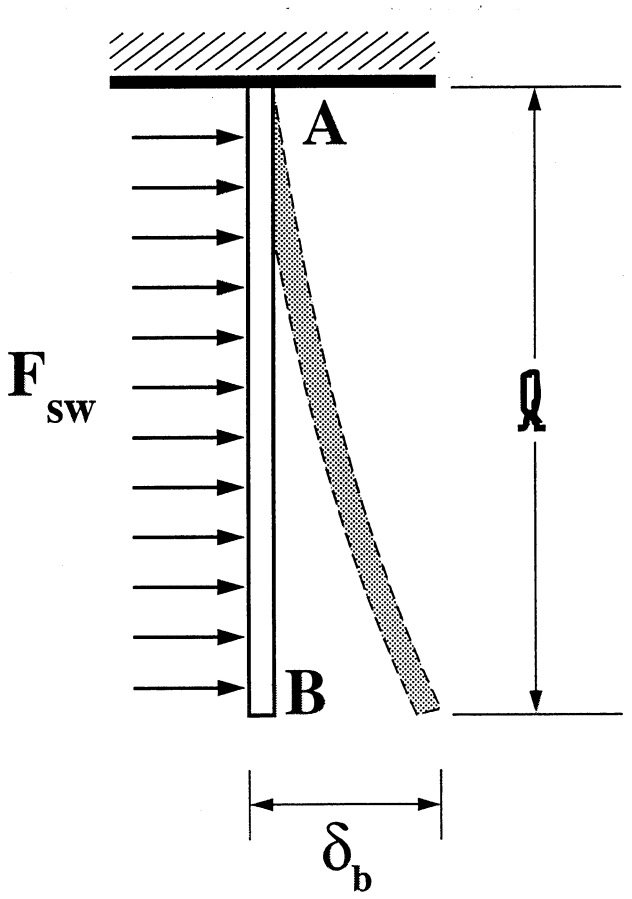

Figure 8. Deflection of a cantilever beam with a uniformly distributed load.

Maximum deflection at point B is given by

$$\delta_B = \frac{F_{SW}\ell^4}{8EI} \qquad (3)$$

Thus, assuming that F_{SW} can be determined using Equation 1 and the hydrophone, and that δ_B can be evaluated using image analysis, the flexural rigidity EI can be obtained. Assuming the following parameters:

- RMS Acoustic pressure, p_0: 200 kPa
- Sound velocity in water at room temperature, c: 1480 m/s
- Density of water, ρ_0 : 1000 kg/m^3
- Fiber radius, a: 25 μm
- Acoustic wavelength, λ: 10 mm

the predicted acoustic force per unit length, F_{SW}, at h = λ/8 is 5.6 x10^{-6} N/m (see Eq. 1). Using Tam Doo and Kerekes[3] flexural rigidity results for earlywood and latewood fibers (Kraft pulp, unbeaten), one can predict the following deflections for 2 mm fibers:

- δ_{early} = 1.2 μm (EI = 9.3 x 10^{-12} Nm^2)
- δ_{late} = 0.4 μm (EI = 26 x 10^{-12} Nm^2)

A three-dimensional translation system located above the acoustic cell was used to position a steel rod anywhere in the acoustic field. Never-dried fibers were attached to the rod using a clamping device. Fibers were imaged using the CCD camera.

Observations using Loblolly Pine fibers indicated that contrary to expectation, fibers did not generally deflect when the acoustic field was turned on, even though the acoustic power did not seem to be a limiting factor. Figure 9 illustrates typical observations. We found that some fibers could not sustain the intensity of the acoustic load; they experienced damage within a few seconds of exposure

(see top-right and bottom-left images). Although not fully explored, we made the assumption that the breaking points were associated to defects in the fibers. It was also observed that just before separation, fiber tips, now presumably subjected to acoustic streaming, were capable of inducing mechanical deflection of remaining fiber sections (see top-right image). Also, we observed some fibers with induced vibrations (see bottom-right image).

The following interpretation is proposed to explain the behavior of cantilever-mounted fibers in the acoustic field. Considering that wood pulp fibers have viscoelastic properties, lack of relaxation time during each oscillation (150,000/sec) of the acoustic field will induce an apparent increase of stiffness, which will lead to an increase in fiber brittleness. Thus, instead of bending, fibers will break. One should note that the increase in fiber brittleness is not permanent and will disappear upon removal of the acoustic field. Also, fiber stiffness under no-cyclic conditions is unaffected. Thus, bending under mechanical loading conditions can still occur (as seen in Figure 9 - top-right image).

We have here a possible basis for the concept of acoustic refining. It has long been thought that an acoustic field could deliver enough power to cut fibers and induce fibrillation.

It is of interest to establish a parallel with the use of an acoustic field to reduce the size of laser ink particles (ultrasonic deinking).

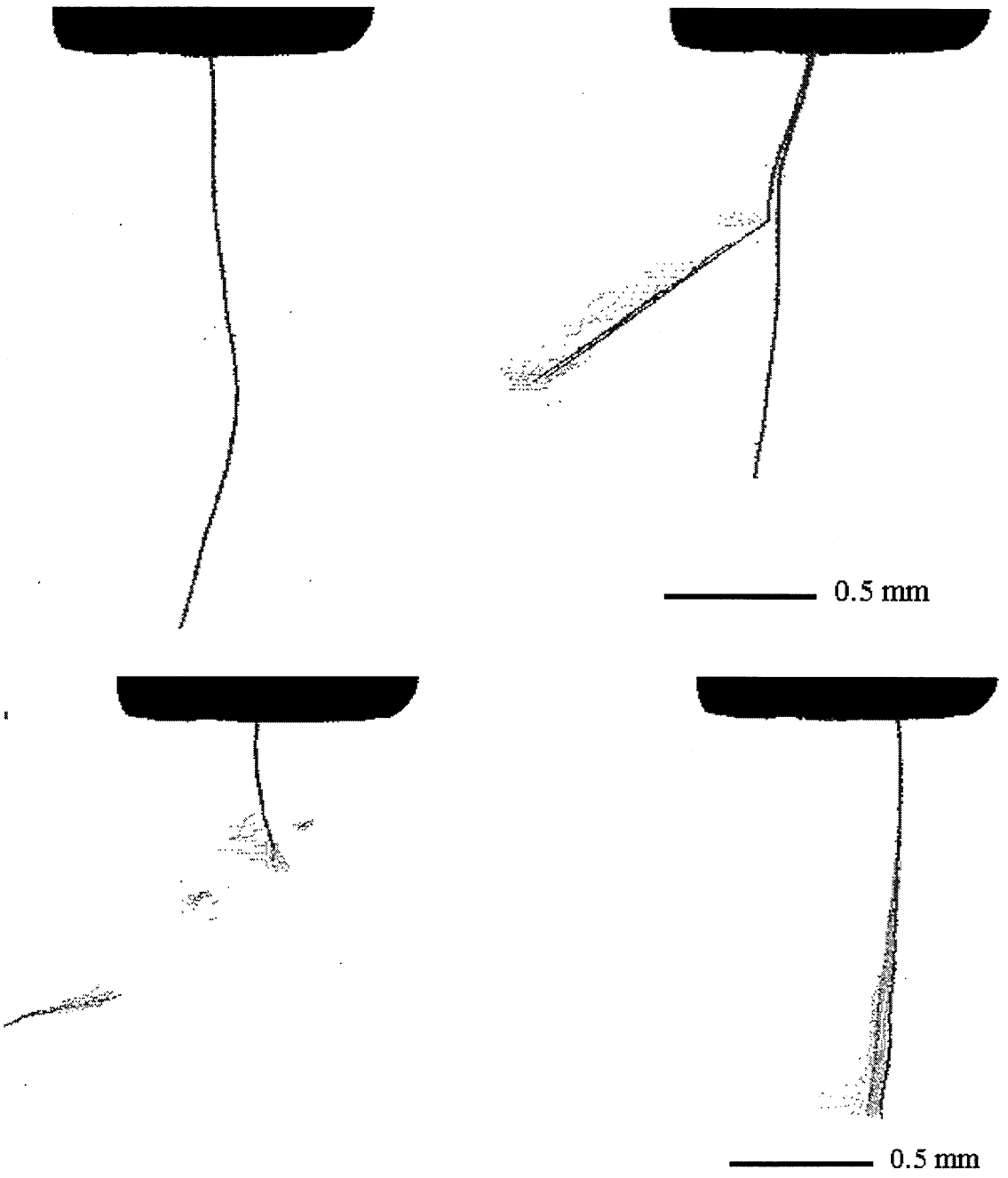

Figure 9. Typical image analysis results of wet fiber flexibility experiments (counterclockwise from top left corner: undeflected fiber when the acoustic field is on; broken fiber; fiber tip removed by acoustic streaming; vibrating fiber).

ACOUSTIC COMPACTIBILITY OF A FIBER MAT

Considering that the concept of acoustic wet fiber flexibility did not work as expected (although we obtained evidence of refining), it was decided to abandon single-fiber testing and move ahead with the investigation of another concept related to flexibility. It was long thought that one might be able to get some very useful information about the compactibility of a fiber mat using a traveling wave field.

The concept is illustrated in Figure 10. A fiber suspension is first transferred to the acoustic cell using the flow system (see Figure 1). Then, assuming that the suspension is at rest (zero flow) in the acoustic cell, the field is turned on. Depending upon fiber flexibility and the intensity of the acoustic power, the suspension will slowly or rapidly compact against the absorber. One can denote the cross-sectional area of the fiber mat by A. While it is hypothesized that this area is related to the degree of compactibility of the fiber mat (at constant acoustic power), it is also sensitive to consistency. In order to eliminate the consistency dependency, we can go a step further and turn the field off. The fiber mat will then spring back. Denoting the new cross-sectional area by A', one can relate the degree of compactibility to the differential cross-sectional area ΔA or compaction area, i.e., A' - A.

The concept was demonstrated using bleached Kraft softwood fibers beaten to several frenesses using a Valley beater. A schematic of the experimental setup is shown in Figure 11. The imaging system was used to record areas A' and A, and compute Δa. Figures 12, 13, and 14 show selected photographs of compacted fiber mats (acoustic power on, A; acoustic power off, A'; Xor operation, ΔA) For comparison, the acoustic power is constant (30 W_{RMS}). The nonuniformity of the fiber

mats is directly related to the transducer's nonuniformity (this problem can be solved by using a more uniform transducer). When compared to the suspension consistency, the fiber mat consistency is about 1.5 to 2 times higher (it could be more with more power). A closer look at Figures 12 and 13 indicates that the fiber compaction is higher as the beating time is increased (higher ΔA).

The compaction area as a function of beating time is plotted in Figures 15 and 16 for two different power levels. Each plot includes results obtained for two different consistencies (0.5 and 1%). While results do not appear to depend on consistency, one can clearly see that the compaction area increased as the beating time is increased. One might expect to gather more conclusive results having a better quality transducer and more power. Also, additional experiments are required to further understand the relationship between compactibility (flexibility) and refining, and to optimize the system.

The concept of acoustic compactibility is of particular interest because it could readily be implemented for on-line monitoring of refining. Dilution and degassing would not be required.

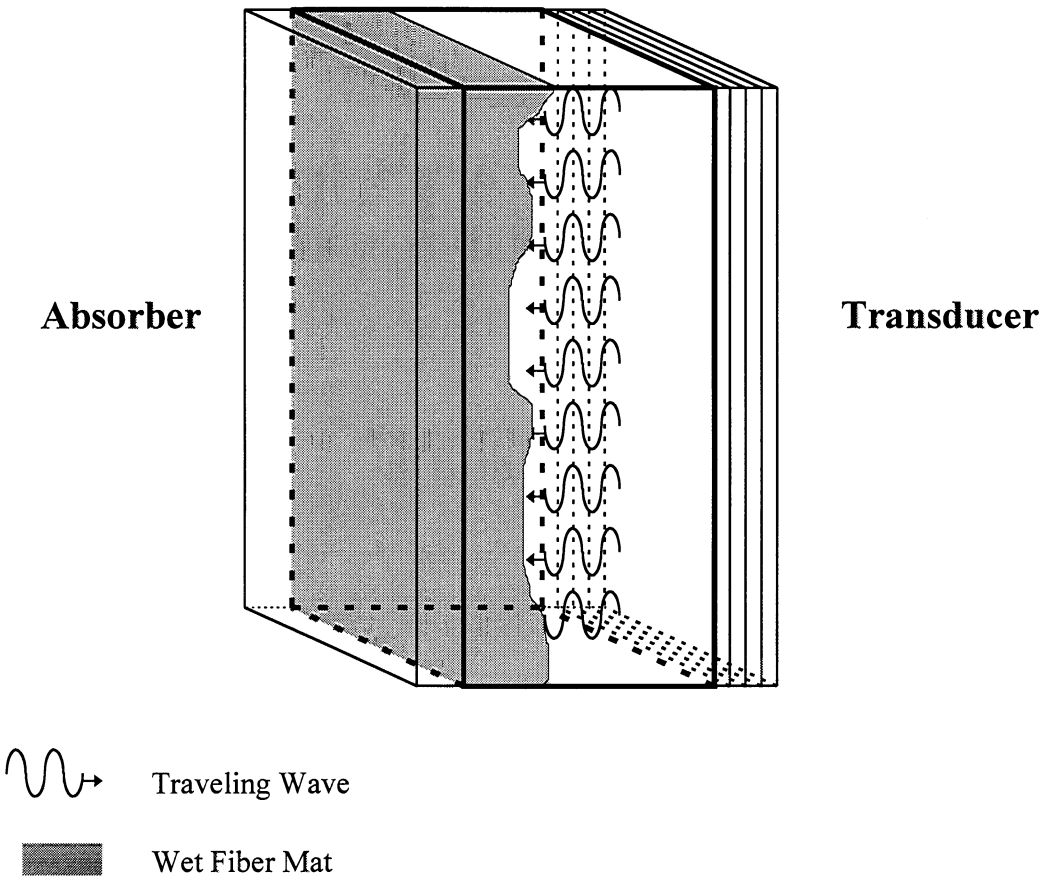

Figure 10. Acoustic compactibility of a wet fiber mat.

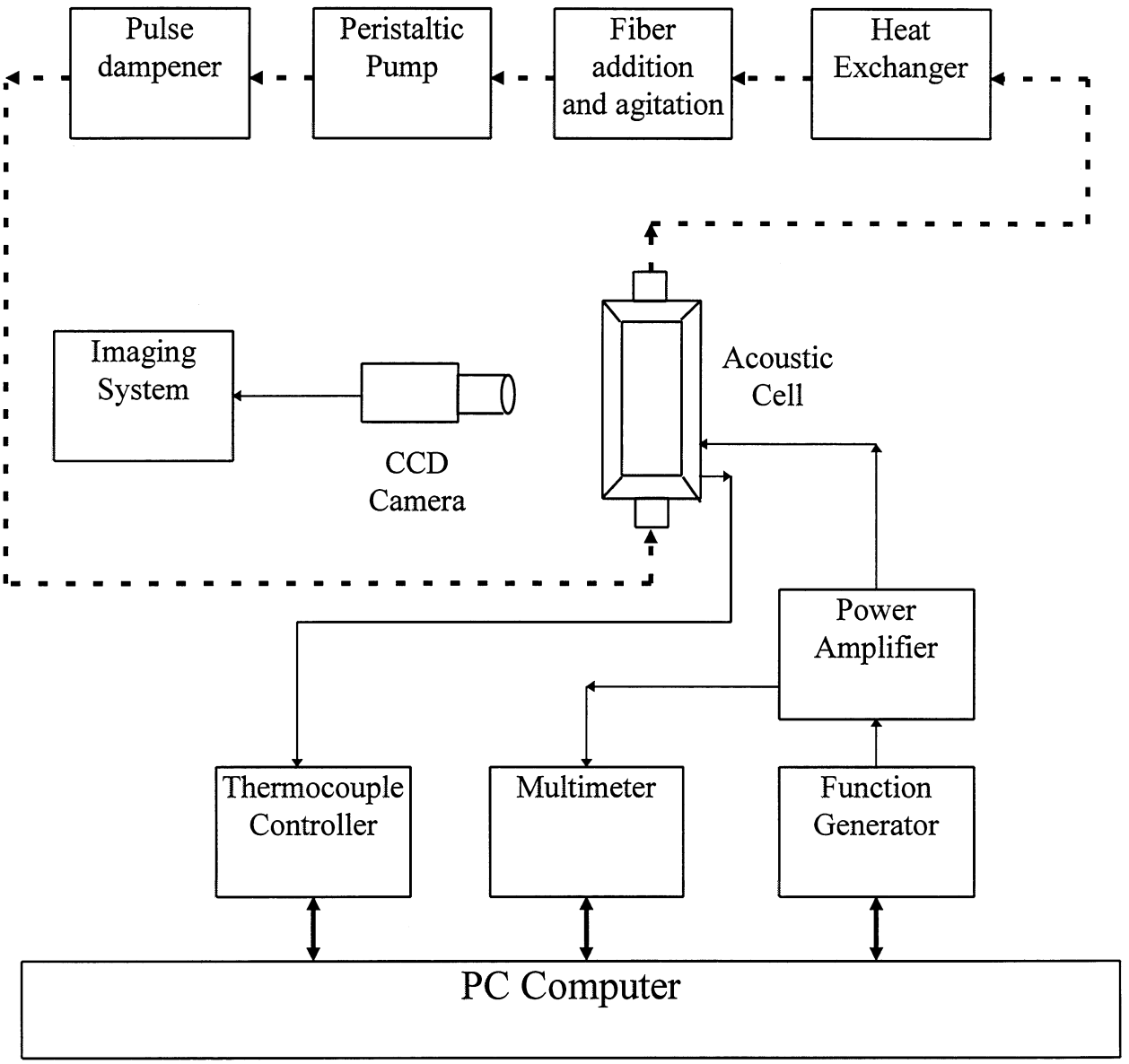

Figure 11. Schematic of the experimental setup for acoustic compactibility experiments.

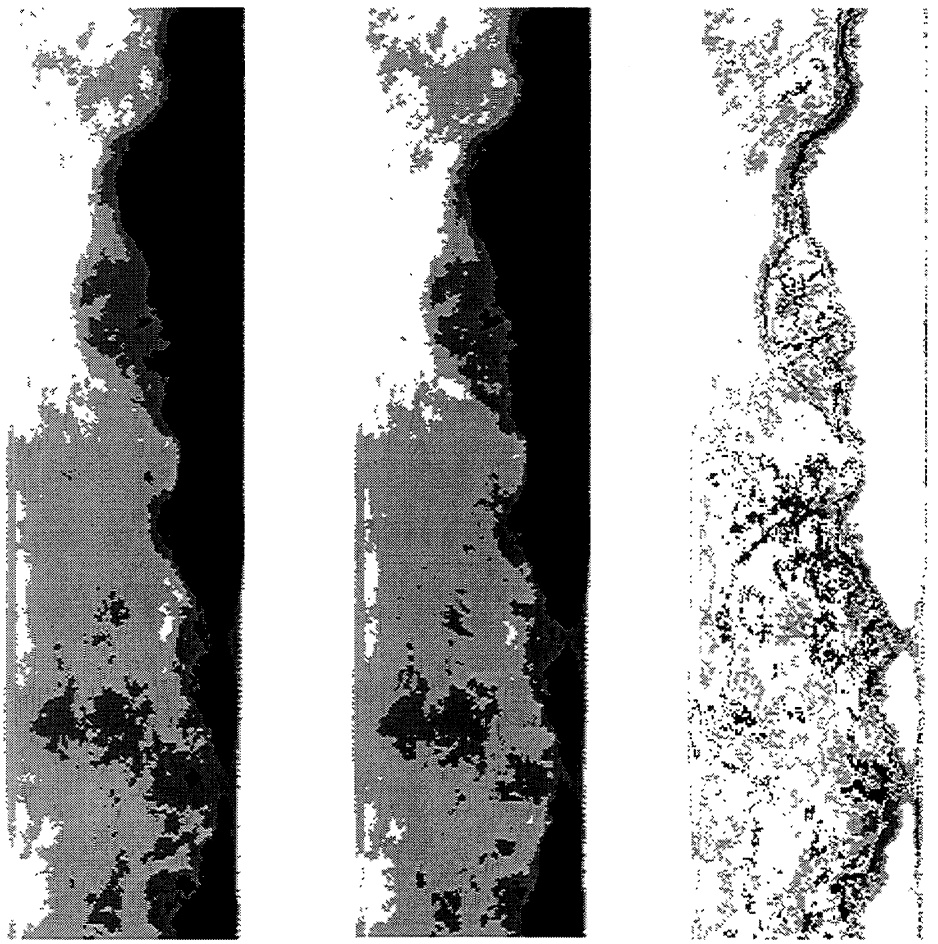

Figure 12. Images of the fiber suspension in the acoustic cell. Testing conditions are 1% consistency, 5 minutes beating, and 30 W_{RMS} acoustic power.

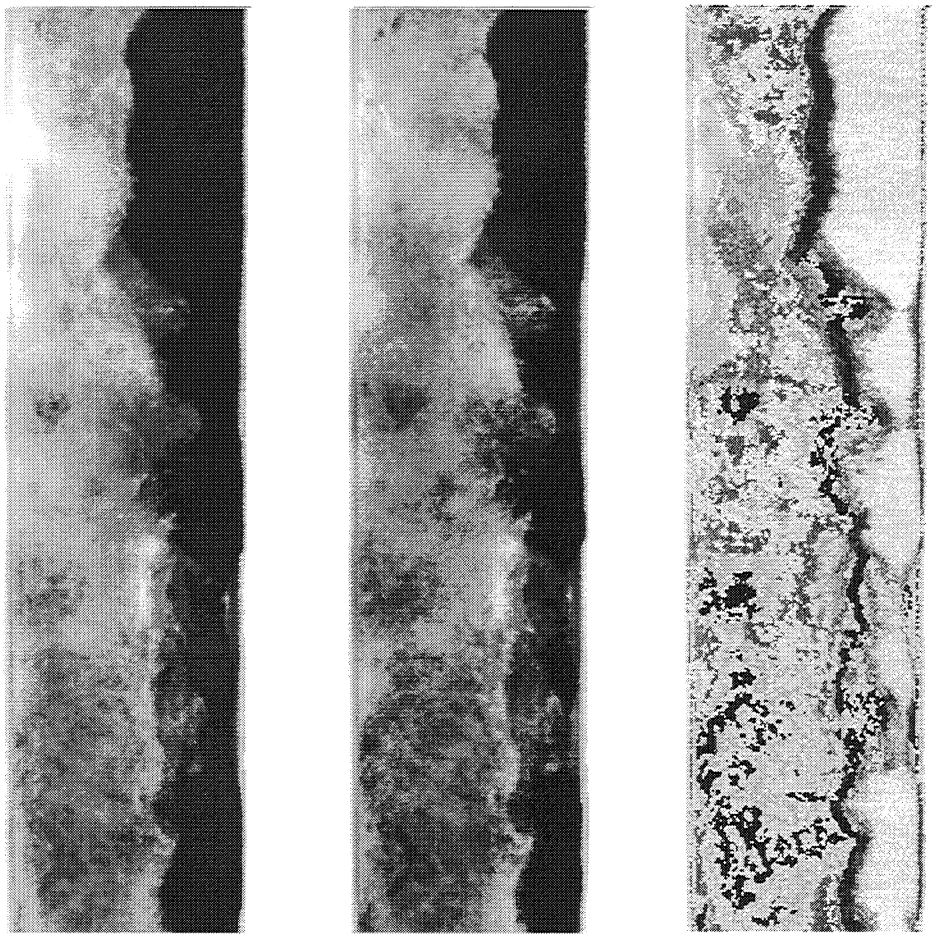

Figure 13. Images of the fiber suspension in the acoustic cell. Testing conditions are 1% consistency, 20 minutes beating, and 30 W_{RMS} acoustic power.

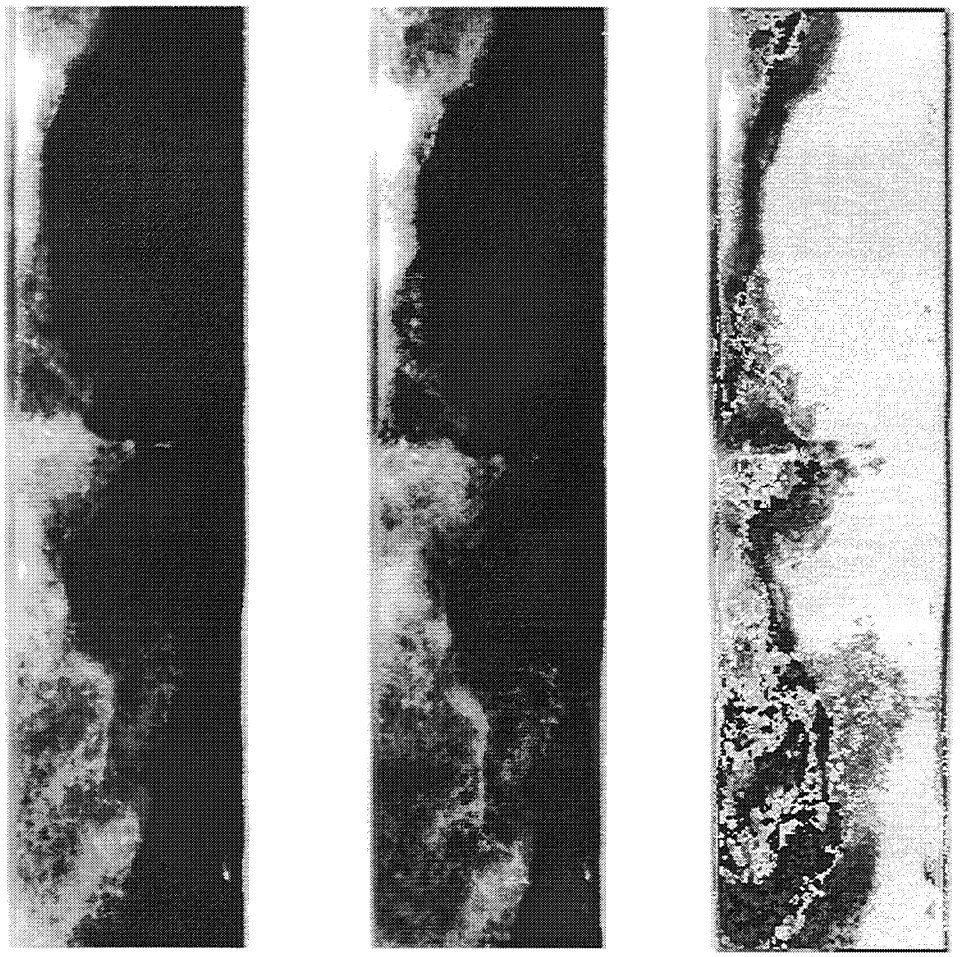

Figure 14. Images of the fiber suspension in the acoustic cell. Testing conditions are 0.5% consistency, 20 minutes beating, and 30 W_{RMS} acoustic power.

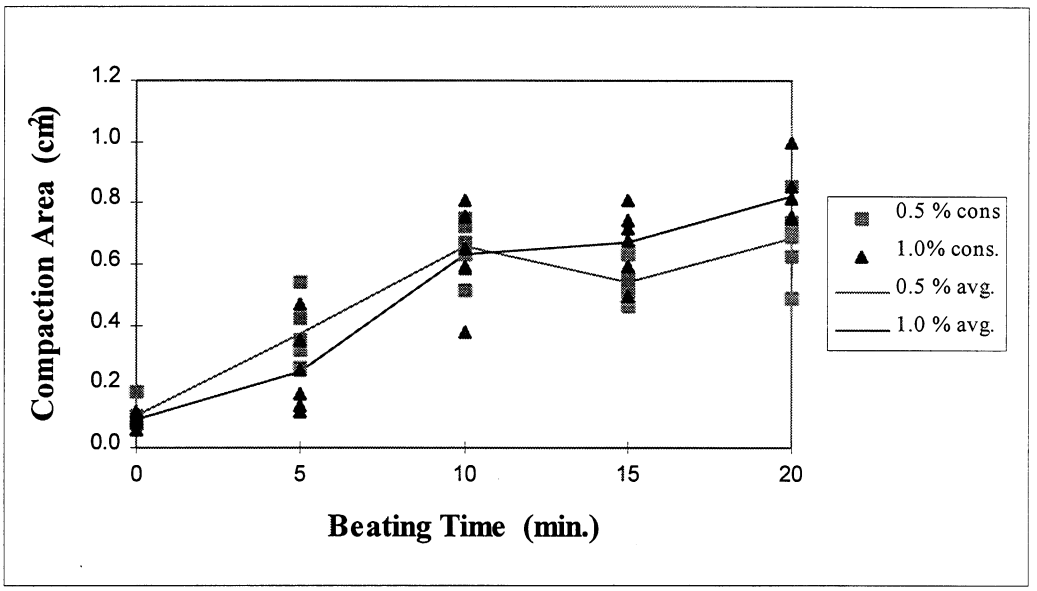

Figure 15. Plot of the compaction area vs. beating time for two different consistency levels. The RMS acoustic power is 20 W.

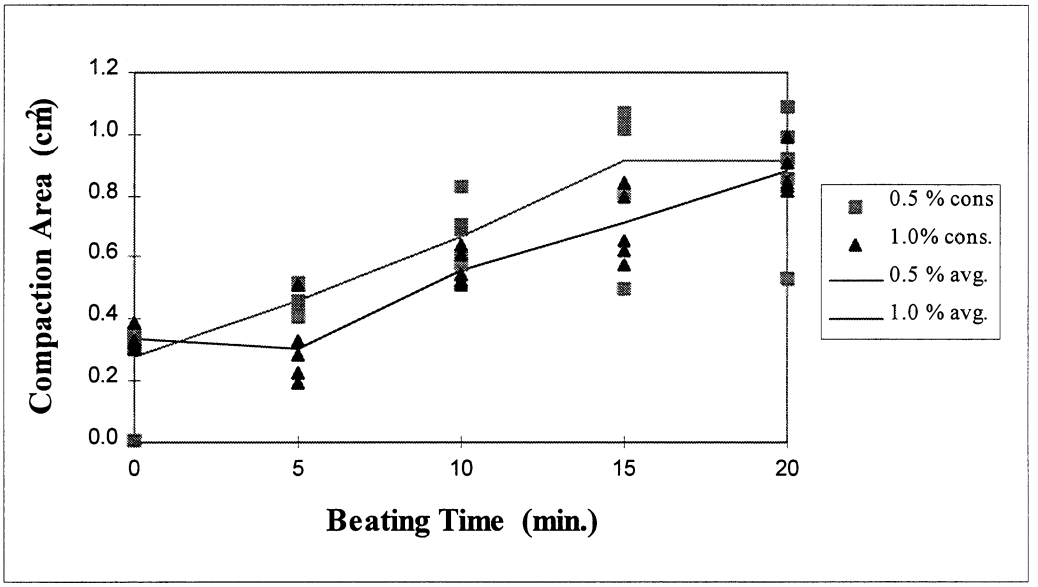

Figure 16. Plot of the compaction area vs. beating time for two different consistency levels. The RMS acoustic power is 30 W.

ACOUSTIC FIBER SEPARATION/FRACTIONATION

Consider a rigid cylindrical particle of radius a free to move in a traveling wave field in which the wave normal is perpendicular to the axis of the cylinder. A derivation of the acoustic force acting on the cylinder was obtained by Awatani:[4]

$$W = \frac{SE}{2(ka)^2}\left[2(w_{0r}R_2 + w_{0s}I_2) + \sum_{m=0}^{\infty}\left\{m(m+1) - e_m(ka)^2\right\}\left\{R_m R_{m+1} + I_m I_{m+1}\right\}\right] \qquad (4)$$

where

$S = \pi a$: Projective area of the cylinder;

$E = \rho_0 k^2 A^2 / 2$: Energy density of the field;

k : Wave number;

A : Amplitude of the acoustic field;

ρ_0 : Density of the suspending medium.

Other parameters in this equation are tedious functions of Bessel and Hankel's functions. In his paper, Awatani supplied a plot of *W/SE* vs. *ka* for various cylinder densities. Assuming that k is constant, it was shown that the acoustic force increases as the radius increases. This is also the case for the acoustic force acting on a rigid cylinder in a standing wave field (See Equation 1).[2]

The dependency of the acoustic force upon the cylinder radius is the basis for the separation technique. Accordingly, the larger is the cylinder radius, the larger is the acoustic force, and hence, the larger is the migration process in the acoustic field. Thus, one should expect coarser wood pulp fibers to agglomerate at a faster rate than slender fibers and/or fines. One should mention that the

dependency of the acoustic force upon the cylinder wall thickness is not considered in Awatani's treatment.

In order to demonstrate the concept, the experimental setup was modified to operate in a batch mode. A schematic of the separation system is shown in Figure 17. The top transparent viewing section in Figure 1 was replaced by a section containing an adjustable mechanical divider with two output streams. An absorber was installed in the acoustic cell to optimize the propagation of a traveling wave field (see above Section on compactibility). The system is not pressurized.

The maximum available flow rate was found to be approximately 1450 ml/min. The maximum acoustic power was limited to 30 W_{RMS} to extend the life of the transducer (Note: after two years of intensive use, the prototype transducer clearly shows signs of rapid deterioration and is no longer as effective as it used to be).

After several unsuccessful trials (the mechanical divider was modified three times), we were able to get the system working in a satisfactory manner. Some problems, which are somewhat related to the small scale of the system, still exist. For instance, if the acoustic power is too high for a certain flow rate, agglomerating fibers are held against the absorber by the acoustic force and do not exit the acoustic cell. Eventually, large chunks of fibers will accumulate and will be removed by the flow. This "sticking" problem is attributed to the rubbery surface of the absorber. It can be partially alleviated by spraying a thin film of Teflon on the absorber's surface.

Figures 18 and 19 show photographs of rayon fibers circulating in the acoustic cell and the divider section when the acoustic field is off and on. Fiber length and denier are 3.2 mm and 3, respectively. The consistency is 0.25%, and the flow rate is 1000 ml/min. One can easily see in Figure 19 the

agglomeration process in the acoustic cell as fibers are moving upward. Output streams have different consistencies.

Other qualitative observations were obtained using softwood and hardwood fibers at consistencies up to 0.5%. Video recordings are available.

Experiments are now underway using a matrix of rayon fibers (different deniers and lengths) to optimize the system. Effects of flow rate and acoustic power are studied. The separation efficiency is also determined. Another series of experiments is scheduled to begin soon using classified wood pulp fibers. Satisfactory progress may be hindered by the poor performance of the transducer.

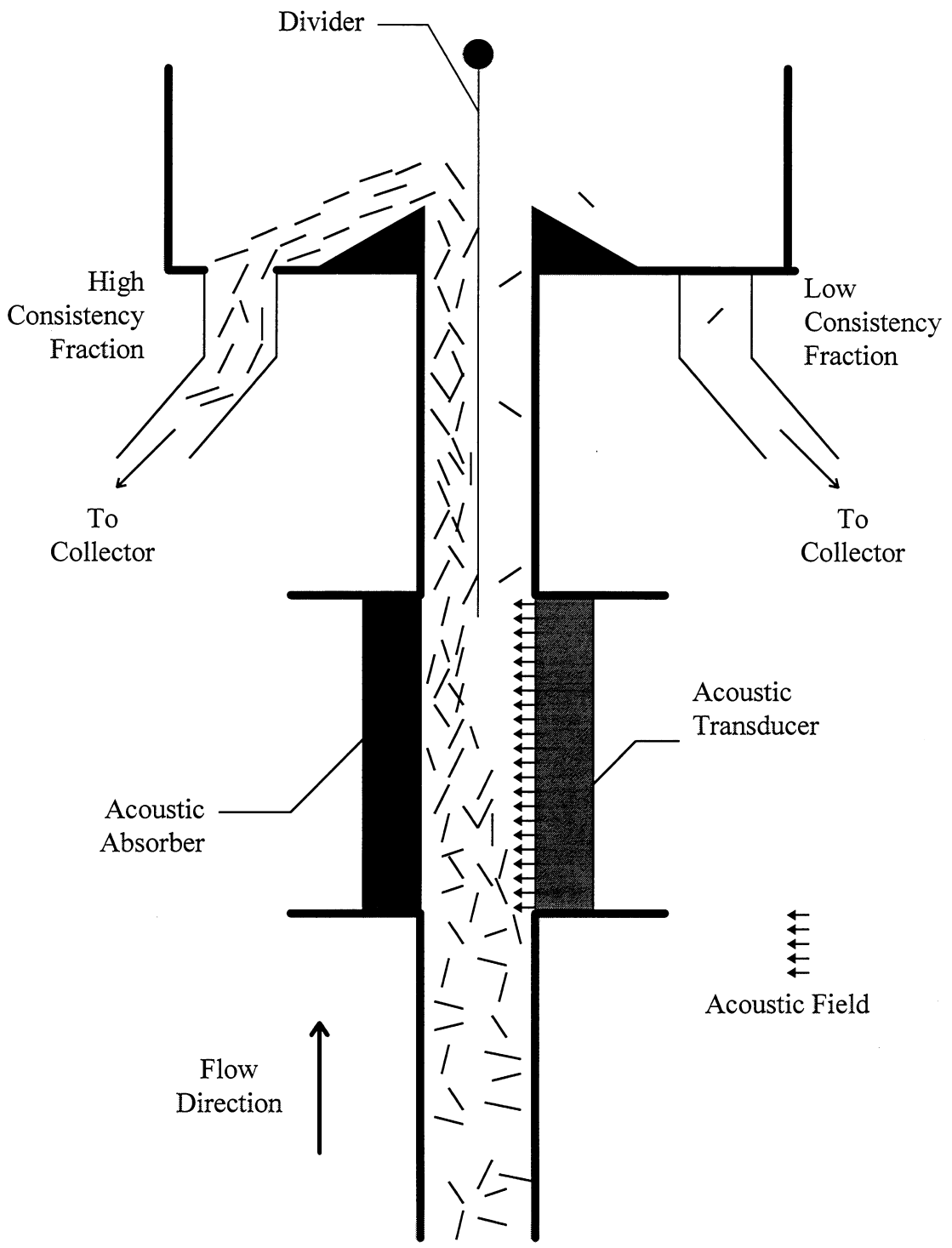

Figure 17. Schematic of the separation system using a traveling wave field.

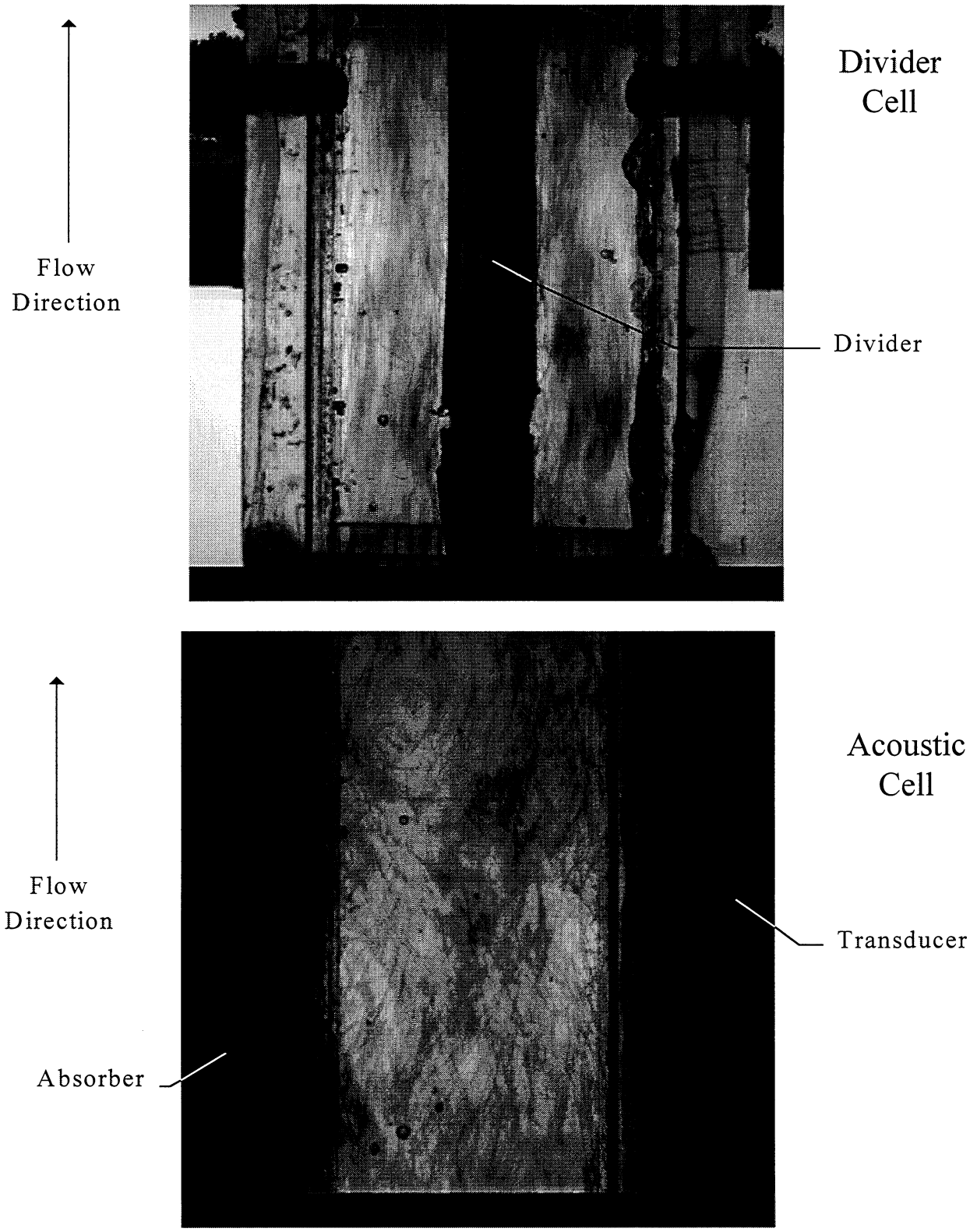

Figure 18. Photographs of acoustic cell and divider section when the acoustic field is off.

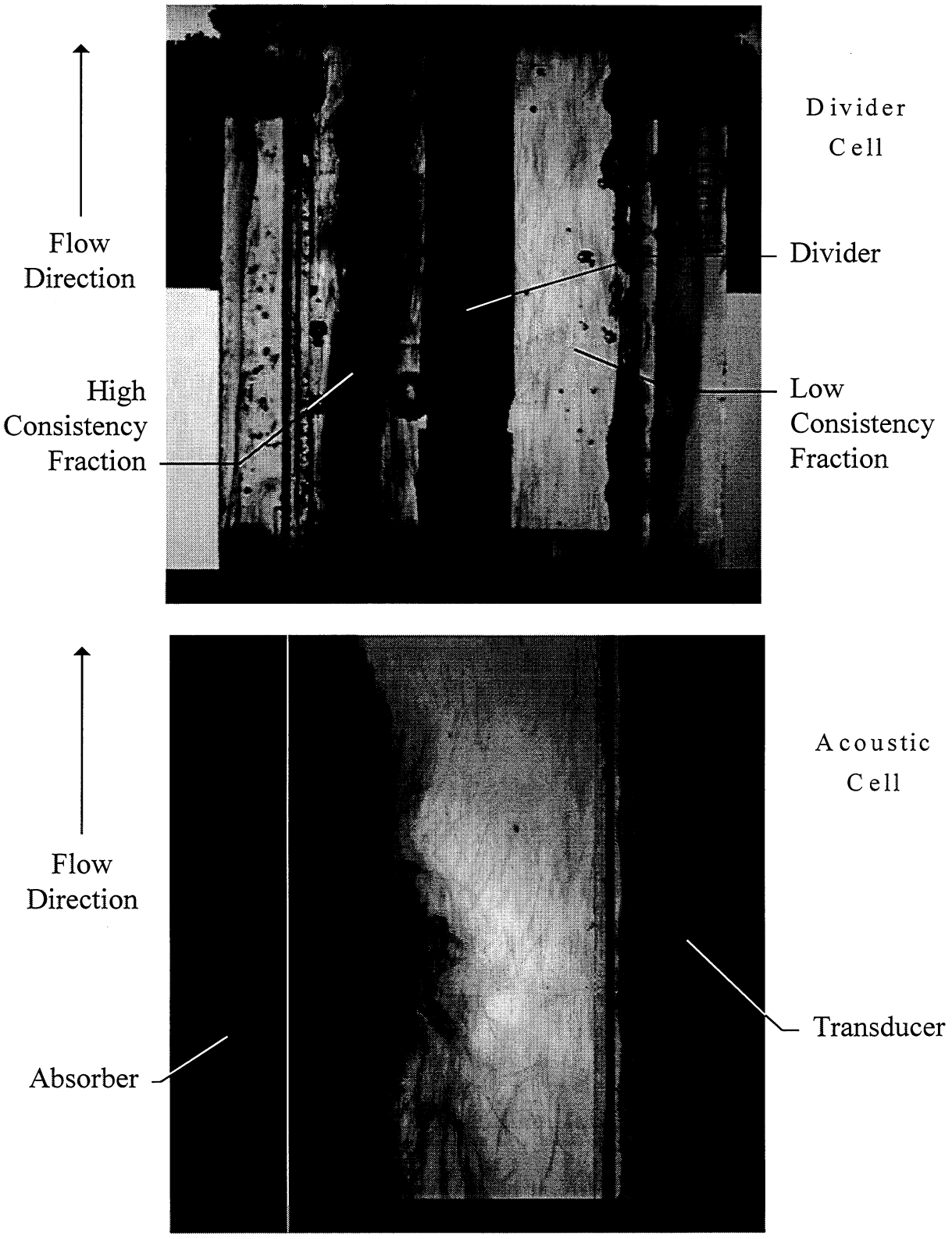

Figure 19. Photographs of acoustic cell and divider section when the acoustic field is on.

ACOUSTIC FIBER AGGLOMERATION AND REORIENTATION

A. Optical Monitoring Systems

Information concerning the amount of agglomeration, speed of agglomeration, as well as rotation of wood pulp fibers due to the acoustic field is determined with a continuous wave laser and polarized light. Figure 20 shows one of the optical system setups that is currently being used.

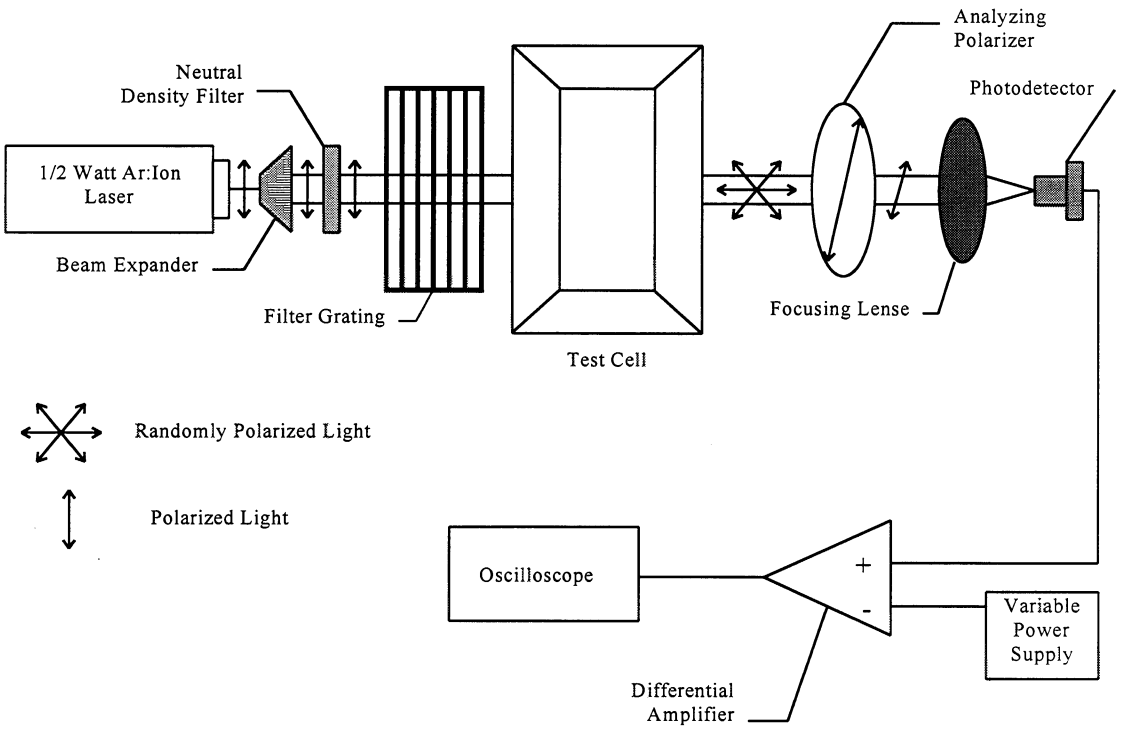

Figure 20. Schematic of one of the optical monitoring systems used to study acoustic agglomeration and reorientation.

Polarized light is supplied by a single-mode, half-watt, Ar:Ion laser operating at the 514.5 nm line. The light is expanded using a beam expander to give roughly a 1 inch diameter beam. The beam then travels through a neutral density filter used to control the laser intensity at the

photodetector. As agglomeration is expected to occur at specific areas in the test cell, a filter grating is inserted into the beam path just before the test cell. This filter grating allows light to enter the cell only at places in which agglomeration will occur. When the polarized light enters the test cell, it is scattered by fibers in the cell and exits with a random polarization. An analyzing polarizer oriented perpendicular to the initial polarization axis is used to remove any photons which were not scattered in the test cell. Those photons which pass through the polarizer are collected by the focusing lens and picked up by the photodetector. The output from the photodetector becomes one of the inputs to a differential amplifier. The second input to the amplifier is a variable power supply. The differential amplifier subtracts the two input signals, and provides an output which is viewed on an oscilloscope.

A second optical system that is being used to determine rotation of fibers is similar to the setup in Figure 20, except a quarter wave plate is inserted between the neutral density filter and the filter grating. The quarter wave plate rotates the laser's polarization to make it circular. Hence, when the laser enters the test cell, the light is circularly polarized. As the light passes through the test cell, it is scattered by the fibers. The analyzing polarizer is again used, except this time it is rotated through 360 degrees, and measurements of the amount of light entering the photodetector are made during the rotation.

B. Current Experiments Being Done Using the Laser Data Acquisition System

Two types of experiments are currently being done using the laser data acquisition system. The first type of experiment is to determine the speed at which fibers are agglomerating. The second type of experiment is to measure the amount of and speed of rotation the fibers undergo during

agglomeration. As of now, we are still acquiring the final pieces of equipment and fine tuning the optical system. Some encouraging data have been taken using these two techniques, but until the systems are fully up and running, we cannot be sure of our results.

B.1 Speed of Fiber Agglomeration

In this experiment, the system shown in Figure 20 is used. Fiber concentrations around 0.001% are used so as to prevent multiple scattering of single photons in the test cell. A continuous flow of fibers through the cell is made possible by an external flow loop. At the start of an experiment, the acoustic field is off, and fibers flow through the cell at a low flow rate. At time = 0, the acoustic field is switched on, and the output of the differential amplifier is recorded using an HP voltmeter. As agglomeration begins to occur, an increasing amount of light is scattered by the fibers. This scattered light is picked up by the photodetector and is recorded by the voltmeter. After approximately two seconds, the acoustic field is switched off, and the experiment ends. Plots of scattered light versus time are made showing the rate at which agglomeration occurs. We will be using rayon fibers of various deniers and lengths to characterize the acoustic radiation pressure and determine its effectiveness in moving fibers.

B.2 Rotation of Fibers during Agglomeration

In this experiment, the second setup described in Section A is used. Again, fiber concentrations around 0.001% are used to prevent multiple scattering of single photons in the test cell. Continuous flow of fibers at a low flow rate is also again provided by an external flow loop. At the start of the experiment, the acoustic field is on, and fibers are agglomerating into planes. Circularly polarized laser light enters the test cell and is scattered by the fibers. An analyzing

polarizer on the exit side of the test cell is rotated through 360 degrees, blocking certain polarizations of light as it is rotated. Polarizations which are not blocked are allowed to pass though the polarizer and are absorbed by the photodetector. The output from the differential amplifier is measured on the oscilloscope, and plots of transmitted light versus polarizer angle are made. In this experiment, we hope to show that as the fibers are rotated in the acoustic field, the polarization of the light exiting the cell also rotates. We can then use the rotation of the polarization to monitor fiber rotation.

Measurements of rotation versus time are also possible with the second setup of Section A. In this case, the analyzing polarizer is set at a specific angle, and the output of the differential amplifier is recorded over time using the HP voltmeter.

We will be using rayon fibers of various deniers and lengths to characterize the acoustic radiation pressure and its ability to rotate fibers.

LITERATURE CITED

1. Frazer, L., Good Vibrations - Extraordinary Advances in Sound-Research Technology, Delta Sky Magazine, 112-119 (January 1995).

2. Brodeur, P., Motion of Fluid Suspended Fibers in a Standing Wave, Ultrasonics 29 301-307 (1991).

3. Tam Doo, P.A. and Kerekes, R. J., A Method to Measure Wet Fiber Flexibility, Tappi J. 64(3) 113-116 (1981).

4. Awatani, J., Study of Acoustic Radiation Pressure (IV) (Radiation Pressure on a Cylinder), Memo. Inst. Sci. Ind. Research Osaka Univ. 12 95-102 (1955).

ON-LINE MEASUREMENT OF PAPER PROPERTIES

STATUS REPORT

FOR

PROJECT F007/3942

Maclin Hall
Ted Jackson
Pierre Brodeur

March 21 - 22, 1995

Institute of Paper Science and Technology
500 10th Street, N.W.
Atlanta, Georgia 30318

TECHNICAL PROGRAM REVIEW

Project Title: ON-LINE MEASUREMENT OF PAPER PROPERTIES
Project Code: ONLIN
Project Number: F007/3942
Division: Engineering and Paper Materials
Project Staff: Mac Hall, Ted Jackson, Pierre Brodeur
Project Budget: $147,000

OBJECTIVE

This project is focused on the fundamentals of paper stiffness measurement and the relationships of ZD and in-plane stiffnesses to on-machine process parameters. It supplements the project to develop commercially viable sensors and instrumentation capable of measuring the velocity of ultrasound in the in-plane and thickness directions of the paper web as it is being made on the paper machine.

SUMMARY

1. Work supported by Cooperative Agreement No. DE-FC05-93CE40006, U.S. Department of Energy, and by the member companies of the Institute of Paper Science and Technology has been completed. The central purpose of this grant was to plan and establish a project to develop a commercially viable system for on-machine, out-of-plane, and in-plane measurements of ultrasonic velocities; to install a working system on a paper machine in a host paper mill; to demonstrate the system's capabilities and benefits to the paper manufacturing industry; and to have a vendor committed to providing and supporting the system.

2. A commercialization plan was developed with ABB Industrial Systems Inc. and submitted to a competitive solicitation for proposals from the DOE "Industrial Waste Reduction Program" in December 1993. In June 1994, IPST was notified that the proposal was among those selected for negotiation of a cooperative agreement. Negotiations have continued into January 1995.

GOAL

For cross-machine samples of typical machine-made paper: determine ZD elastic stiffness variations observed with and without deliberate process changes; determine relationship of ZD elastic stiffnesses to in-plane elastic stiffnesses; and determine relationships of elastic stiffnesses to the "strength" measures of short span compression (STFI) and Ring Crush (RC).

BACKGROUND

The variations of the elastic stiffnesses of paper with refining, fiber orientation, wet pressing pressure, wet straining (draws), and drying restraints have been studied and reported (Baum et al., 1984; Habeger and Baum, 1986). These studies have demonstrated that elastic stiffnesses are sensitive to changes in furnish and to changes in various process parameters. In order to separately identify and provide maximum sensitivity to the effects of the various paper machine variables for machine control, the elastic stiffnesses in both the in-plane and thickness directions should be measured. Measurement of these elastic stiffnesses along with the basis weight, moisture, and caliper of the web on the paper machine should provide a means to continuously monitor product quality and to control the paper manufacturing process.

Several of the studies (Baum et al., 1979; Whitsitt, 1985) have noted and made use of empirical relationships between shear and longitudinal ultrasonic velocities. Such relationships are

$(V_{SH,MDorCD})^2 = k_1 [(V_{MD})(V_{CD})]$ for in-plane, and

$(V_{SH,MD-ZD})^2 = k_2 [(V_{MD})(V_{ZD})]$, and $(V_{SH,CD-ZD})^2 = k_3 [(V_{CD})(V_{ZD})]$ for out-of-plane.

In terms of elastic stiffnesses, these relationships imply that the geometric mean of the longitudinal stiffnesses in any plane is proportional to the shear stiffness in that plane. Thus, in addition to the ZD elastic stiffness, the simultaneous measurement of the ZD longitudinal ultrasonic velocity with the in-plane ultrasonic velocities may also provide an on-machine measure of the ZD shear stiffnesses.

DISCUSSION OF EXPERIMENTAL MEASUREMENTS

The measurement of in-plane elastic stiffnesses on cross-reel strips is now an accepted practice in many mills. However, very little has been done to evaluate the ZD stiffness variation of cross-reel strips. Are the measurable cross-machine variations significant? Are the variations within a reel and between successive reels or successive shifts significant? Can significant variations be related to process changes? Many of the previous studies have involved papers made in the laboratory under selected conditions. The predicted relationships of the elastic stiffnesses to the various paper machine variables for machine-made papers need to be confirmed, particularly for the ZD stiffness.

With the long-term objective of proving the usefulness of the elastic stiffnesses for process control, arrangements have been made to obtain various *cross-reel-strip samples* of Neutral Sulfite Semichemical (NSSC) medium along with in-plane ultrasonic data and operating conditions from the mill. Initial emphasis will be on determining what samples, mill information, physical testing, and analysis is most appropriate to provide information for the long-term objective. The in-plane ultrasonic data will be reviewed to select specific CD positions with different, extreme MD and CD values. Samples from these positions will be tested and evaluated for correlation of elastic properties with known operating conditions and with strength properties (CD ring crush, MD Concora, STFI compressive strength).

After analyzing the initial result to determine the most promising sampling and data collecting procedures, additional samples will be requested with the intention of measuring elastic stiffness changes resulting from specific process changes.

A few *extended, web-wide samples* will also be requested. These samples will be used to determine the short range variations of the elastic stiffnesses along the machine direction of the web. The samples will also be used to demonstrate the measurement data that would be

available to the papermaker from on-machine ZD and in-plane ultrasonic instruments mounted in a scanner at the dry end of the paper machine.

The *extended, web-wide samples* will be full cross-machine width and ~300 feet long. The process settings that may be available, and the basis weight (BW), caliper, and moisture data from the scanner will be obtained when each sample is taken. Each sample will be slit into strips, 12 inches wide by ~300 feet long in the MD. The strips will be spliced end-to-end to form a roll to run on the IPST web handler. The sample from the paper machine would be a small diameter, very wide roll much like a roll of carpet. It is hoped that the mill might convert this into a manageable series of roll widths for transport using the jumbo-to-daughter roll conversion equipment.

The cuts should be at integral footage from the web center. For example, if the trim width is 310 inches (about 26 feet), the sample could be cut in the center and at 4 and 8 feet on each side of the center. This would give a series of roll widths: ~5,4,4,4,4,~5 feet. The front and back edges would be left untrimmed from jumbo roll. The smaller width rolls will be sent to a converter for slitting into 12-inch wide strips. The cut and slit segments will need to be marked so that their front-to-back sequence can be reconstructed.

Measurements that will be made on each 12-inch wide sample "roll" are

a. ZD velocity and Measurex (MX) caliper in the center and ±4 inches on each side of the center. This will provide ZD velocity and caliper data every 4 inches across the web.
b. When the ABB scanner is in place and operational, basis weight and moisture can be added to the data every 4 inches across the web.
c. In-plane measurements: MD Shear and CD Longitudinal and ±45 degrees for polar angle.

A composite of the data will be plotted as a demonstration of on-machine scan. Data will also be used to calculate CD STFI and CD Ring Crush, using Whitsitt formulas.

The experiments described above will be repeated with samples from a paper machine making linerboard.

TOWARD COMMERCIALIZATION

The Department of Energy (DOE), Office of Industrial Technologies (OIT), sponsored a solicitation for Cooperative Agreements as part of its Industrial Waste Reduction Program in September 1993. This solicitation was focused on the metals industry and the pulp and paper industry. The program targeted key waste reduction opportunities that offered significant material, energy, and cost savings, and environmental benefits. The solicitation required industry participation and 50% cost sharing. Working with ABB and with the concurrence of the Herty Foundation Center in Savannah, Georgia, a plan to aggressively pursue commercialization was prepared, and IPST submitted a cost-share proposal to DOE by the solicitation due date, December 2, 1993.

The proposed program involves a cooperative effort between the Institute of Paper Science and Technology (IPST) and ABB Industrial Systems Inc. (ABB). Additional participants will be the Herty Foundation Research and Development Center with sensor and system testing on its new pilot paper machine and a paper manufacturing company selected to provide a Host Mill with a paper machine and support for "Beta Site" evaluation of the developed sensors and instrumentation.

Pilot-scale prototype and full-scale proof-of-principle units, for both in-plane ultrasonic velocity measurements and out-of-plane (ZD) ultrasonic velocity measurements, will be built and tested. Packaging paper and paperboard are the principal target applications because mechanical properties are of primary importance in the end-use of these products. The pilot-scale prototype units will be tested at IPST and at Herty. The full-scale proof-of-principle units will be verified at IPST and Herty and demonstrated on a paper machine in an actual commercial production environment in a Host Mill.

The ultimate objective is to commercialize on-machine ultrasonic velocity sensors to provide real-time data for improved control of the papermaking process. Extensive on-machine testing and performance demonstration is anticipated as a requirement to gain acceptance by the paper industry. A 4-year development and testing program was proposed to ensure that the developed measurement and control instrumentation is a commercially viable system. Funds were requested from DOE for the 4-year program with cost-sharing by IPST, ABB, Herty, and the Host Mill, such that DOE's share would not exceed 50%.

In June 1994, IPST was notified that the proposal was among those selected for negotiation of a cooperative agreement. Negotiations have continued through January 1995.

REFERENCES

Baum, G.A., Brennan, D.C., and Habeger, C.C., "Orthotropic Elastic Constants of Paper," *Tappi J.* 64 (8):97(1981).

Baum, G.A., Pers, K., Shepard, D.R., and Ave'Lallemant, T.R., "Wet Straining of Paper," *Tappi J.* 67 (5):100(1984).

Habeger, C.C., and Baum, G.A., "On-line Measurement of Paper Mechanical Properties," *Tappi J.* 69(6): 106(1986).

Whitsitt, W.J., "Relationships Between Elastic Properties and End-Use Performance," Project 2695-23, Report One, A Progress Report to the Fourdrinier Kraft Board Group of the API (January 30, 1985).

DIMENSIONAL STABILITY

STATUS REPORT

FOR

PROJECT E00102

Douglas W. Coffin

March 21 - 22, 1995

Institute of Paper Science and Technology
500 10th Street, N.W.
Atlanta, Georgia 30318

TECHNICAL PROGRAM REVIEW

Project Title: Dimensional Stability

Project Code: DIMSTAB

Project Number: E00102

Project Staff: Douglas W. Coffin

Project Budget: $204,000

OBJECTIVE

The objectives of this project are to develop a science based understanding of the dimensional stability of paper and paperboard, especially the phenomenon of cockle, and to apply these fundamental results to practical industrial problems.

SUMMARY

This project was newly established this year, and work was begun in July of 1994. To focus the efforts of this program to a critical problem in the paper industry, a survey of industry needs in the area of dimensional stability was conducted. From the results of the survey, it was decided that the initial emphasis of the project would focus on the problem of cockle in paper and paperboard. For this research program, cockle is used to describe any out-of-plane displacements created in the sheet due to planar variations of strain which are created by changes in the moisture content of the sheet.

The emphasis of the work completed during the past year was the following: developing a rigorous research program on cockle, collecting and studying previous work on cockle, and developing a fundamental analysis illustrating the mechanisms of cockle. Four tasks were undertaken to build a foundation for the cockle research program. These tasks are as follows:

1. Conduct a critical review of previous work on cockle found in the literature.

2. Develop the analytical capability to predict and study the cockling of paper.

3. Collect samples of cockle to study and classify different types of cockle.

4. Develop an experimental program for studying the formation of cockles in the laboratory.

For task 1, the results of the literature search to date are presented in the section titled Background. It was found that many results and comments based on practical experience can be found in the literature, but little work on the fundamentals of cockle was located. Before this task is completed, more critical analysis of important papers is needed, and the literature must be searched for any other works on cockle.

It is felt that analysis of cockle based on the fundamental concepts of physics and material behavior will lead to an increased understanding of the phenomenon. Preliminary results for a fundamental analysis of cockle are presented in the section titled Analysis. From this fundamental analysis, more realistic models for cockle will be developed.

Because cockle occurs in various situations and cockle is used by the industry to describe many different out-of-plane deformations, a description of the different types of cockle is needed along with a classification system. Some samples have been obtained, but more effort needs to be made this year at obtaining additional samples.

In order to study the formation of cockle under controlled situations, a laboratory simulation of cockles is needed. In addition, experimental results could be used to verify numerical results. Due to the expected difficulty in controlling the formation of cockles in the lab, this task is being delayed so that information gained from the other tasks can be used to intelligently design an experimental program.

GOALS

The primary goals of this program are to (1) build a science based understanding of cockle in paper; (2) develop scientific and engineering solutions to the cockle of paper in the manufacture, converting, and end-use of paper; and (3) transfer this technology to industry so that cockle problems can be controlled, eliminated, or avoided.

For 1995, the goals of the projectare to (1) complete the critical review of the literature, (2) complete the fundamental analysis of the formation of a single cockle, (3) develop and implement numerical methods for analyzing cockle in paper and paperboard, (4) develop constitutive models that accurately predict the response of paper to applied loads and changes in moisture content, (5) collect samples of cockle and classify types of cockle, and (6) develop an experimental setup to study cockle.

BACKGROUND

In general, cockle in paper and paperboard can be attributed to nonuniform shrinkage and/or expansion in the plane of the sheet. In the 1993 addition of Pulp and Paper Dictionary [1], cockle is defined as "a paper defect appearing as a wrinkle caused by nonuniform shrinking due to uneven drying or sheet formation." The key word in this definition is nonuniform. This definition of cockle is limited to the case of shrinkage due to drying, but in the present program, any out-of-plane deformations due to nonuniform

expansion and contraction in the plane of the sheet are referred to as cockles. In addition to nonuniformity, a change in the moisture content of the paper is a key factor leading to the formation of cockles. Thus, cockles are a manifestation of the dimensional instability of paper.

Cockles are created under many different circumstances, and many factors can lead to cockle. For example, variations in basis weight throughout the sheet or localized wetting and/or drying of the sheet can lead to cockle. It is important to note, though, that on the most fundamental level cockles are caused by nonuniform shrinkage and expansion of the sheet. Cockles may form during the manufacture, converting, or end-use of paper.

Because of the varied situations that lead to cockle, it is one of the most difficult manifestations of paper's dimensional instability and is one of the least understood phenomena in dimensional stability. Cockle has been a long-standing problem in the paper industry. In fact, Smith [2] stated that cockling is "an endemic blemish in paper which has troubled paper-makers since Tsai Lun started the art on its way in 105 A.D." A fundamental study of cockle that addresses the most basic causes of cockle is needed. The information gained in such a study will be beneficial in determining the causes of specific cockle problems so that they can be controlled or eliminated. In the literature, the cockle has not been fully addressed with very little discussion on the fundamental mechanisms of cockle. The literature does reveal, however, that cockle has been a problem for many years and continues to be a problem. Most likely, cockling of paper will be a problem in the future. In the following, the literature pertaining to cockle that has been collected to date is discussed.

Observations of the Causes of Cockle

In 1912, the *Paper Trade Journal* [3] published an article on the causes of wrinkles and cockles. The following causes for cockled paper are given in the article: high degree of beating, nonuniform removal of water, uneven flow of pulp onto the wire, too sudden heating, loose felts, and poor storage conditions. Above all, it was stressed that uniformity is the key factor associated to drying. In fact, the article stated "slow and perfectly uniform drying is the great thing to be aimed at."

Beyond the nonuniform expansion and contraction of the sheet, no mechanisms that lead to cockle were given in this article. Possible mechanisms for cockle were developed later and are discussed in the next section. The remainder of this section discusses the literature that pertains to observations of cockle. It is interesting to note that many of the same factors that were known to contribute to cockle in 1912 [3] still pose problems to the papermaker today.

The 1912 *Paper Trade Journal* article [3] stated that nonuniform delivery of the pulp onto the wire leads to thick and thin regions in the paper. Upon drying, the thinner sections dry faster than the thicker sections and lead to cockling. As recent as 1992 [4], this type of variation has been linked to cockling. Dittmann [4] reported that basis weight variations caused by periodic hydraulic pulsations were found to correlate to cockling in a super calendered paper produced at the Lake Superior Paper Industries mill in Duluth, Minnesota.

Lack of tension in the felts was pointed out as another cause of cockles in the 1912 *Paper Trade Journal* article [3]. This can be interpreted as a lack of restraint during drying. The importance of felts and proper restraint during drying to eliminate cockling have been enumerated many times [5-10]. Wedel [8,9] showed that restraint during drying

could eliminate cockling in fine papers. He showed that increased restraint lead to decreased CD shrinkage as well as decreased cockles. Chance [10] discussed a single tier Bel-Champ dryer section that adds sheet restraint during drying and reduced cockle.

Nonuniformity leading to nonuniform water removal is the main point that comes up in most discussions of cockle. In addition to the articles discussed above, this theme is discussed in references [2, 11-21]. For example, Bell [12] discussed how selective remoisturizing of the sheet can allow for more uniform drying of the sheet and eliminate the formation of cockles in the drier region.

Most of the work referenced above [2-18, 20-21] pertains mainly to cockles formed during the papermaking process. Cockles have also been known to form in paper after it has been manufactured, for example, during storage [3] or printing [19]. Any situation which leads to a nonuniform change in moisture levels may lead to cockle. One of the newest areas where cockle has become a problem is in ink jet printing [19]. The application of ink to large areas of the sheet of paper lead to nonuniformities in shrinkage and expansion, and as a result cockles form. These cockles can be very large, as much as 200 mils for a paper with a caliper of 4 mils [19]. Cockles in ink jet papers cause problems with sheet stacking, aesthetics of the sheet, and moving the sheet through the printer.

Mechanisms of Cockle

As illustrated in the last section, much has been reported on factors that lead to cockle. On the other hand, only limited work can be found which discusses the possible mechanisms of cockle. In 1950, Smith [2] gave an explanation of cockle that has been cited most often in latter works, although some of the underlying concepts of mechanisms that lead to cockle were reported prior to this time.

The work of Stamm [5] is the earliest work from which a mechanism of cockle can be inferred. Stamm stated:

> *Both cockle and curl are fundamentally due to unequal tension in the sheet and this unequal tension is set up in the process of drying. Furthermore, this tension is a direct function of the shrinkage. Thus the greater the shrinkage, the greater the tendency to give you trouble..*

Stamm further discussed that cockle occurs during shrinkage of the fibers, but only after there is ample restraint in the sheet to transmit the forces. Stamm's mechanism for cockle can be considered as follows. First, a condition is created from either nonuniform formation or drying where the sheet contracts in a nonuniform manner. Second, there is sufficient constraint to create "tension" in the sheet. Third, these "tensions" cause the paper to cockle. Stamm's use of tension should be replaced with stresses. In addition, tensile stresses tend to decrease the curvature of a surface, whereas compressive stresses tend to increase the curvature of a surface. Therefore, Stamm's use of the word tension is probably not correct. In addition, Stamm did not state how these "tensions" actually cause the cockle to form; thus, it is an incomplete mechanism to cockle. Along this same line of thought, Shriver [22] hypothesized that cockle was produced by differential shrinkage in the paper and transmission of stress throughout the sheet. Shriver also suggested that cockle would correlate with the rate of drying and variability of single fibers in the sheet.

One of the first in-depth discussions of cockle was given by Smith in 1950 [2]. Smith suggested that cockle is due to the uneven stretching or contraction over the surface of the sheet. Furthermore, he stated that nonuniform shrinkage occurs because of variations in density, variations in water content, and variations in fiber orientation. Smith made the following comments about cockle:

(1) Cockling is merely a visible manifestation of portions of a sheet being changed in length or width in relation to other parts of the sheet.

(2) The main circumstance giving rise to cockling is the shrinkage on drying of paper sheets: this cannot alone cause cockling, however, without secondary circumstance giving rise to irregularity of the shrinkage from place to place. Many of these circumstances are known.

(3) A necessary part of the mechanism of most varieties of cockling is the formation of irregular dried-in strains in the sheet. In some cases, however, the capacity of the sheet to take up a variable dried-in strain enables paper or board free from cockling to be made from a wet sheet having irregular shrinkage properties.

Smith defined dried-in strains as the difference between the potential shrinkage minus the actual shrinkage. The potential shrinkage is the total shrinkage of an unrestrained sheet. The actual shrinkage is less than the potential shrinkage due to restraint from tension during drying. If a patch of a sheet dries faster than the surrounding material, it will undergo more shrinkage and dry under tension. A dried-in strain will exist in the paper, and as the surrounding paper continues to shrink, it will cause the paper to cockle [2].

Although Smith's theory on cockle seems very plausible, it was based only on practical experience and conjecture. In 1955, Brecht [21] and Brecht, Müller, and Weiss [23] presented laboratory results verifying the theory presented by Smith [2]. Moist sheets having uneven distributions of moisture over their surface were dried, which resulted in cockle. Brecht [21] stated that cockles always occurred in areas which were initially

drier, thus, in agreement with Smith's theory. In addition, samples were prepared that had areas with different basis weight. For these samples, cockles always occurred in areas with lower weight or thicknesses, which dried sooner than the rest of the sheet. In addition, Brecht showed that variations in temperature across the sheet result in cockling. Also, Brecht showed that beating of the fibers increases the degree of cockling because beating tends to increase the degree of shrinking. Finally, Brecht found that pressing the paper to the drying surface with sufficient pressure can alleviate the formation of cockles.

The work of Brecht has been the only laboratory experiments on cockle reported in the literature. It definitively showed that cockle occurs due to nonuniform shrinkage across the sheet. Since this time, the descriptions of cockle given by Chodhury [16], Gallay [17], and Uesaka [18] only recap the work of Smith [2] and Brecht [21].

Smith's description of cockle formation did not give an explicit mechanism for the cause of cockle in paper. If paper can support compressive and tensile loads while remaining flat, then paper may be able to accommodate the nonuniformity of shrinkage or expansion without producing cockle. Since paper does cockle, there must be a mechanism which causes cockles to form. A possible mechanism for this is given by Uesaka [18], although he credits Smith [2] with the mechanism. Uesaka [18] states that the initially drier region is subjected to compressive stresses when the initially wetter section shrinks. This compressive stress induces localized buckling of the paper which produces the cockles. The paper will buckle when the compressive stresses overcome the bending resistance of the paper.

Localized buckling is not the only mechanism that has been proposed to explain the mechanism that produces the out-of-plane cockles. Gooray and Agbezuge [19] attributed the out-of-plane displacements to localized curl of the paper. Curl results from

differences in the expansion or contraction of the sheet through the thickness of the paper. As the moisture level changes through the thickness, paper may curl. If this moisture change is nonuniform, cockles will be produced. Kajanto [20] stated that cockle can be caused by local curl of the paper. With the use of a finite-element analysis, Kajanto [20] predicted that a cockled pattern resulted from local variations of the paper's two-sidedness. This type of cockle is due to the coupling between the axial strain and the curvature.

Kajanto [20] also investigated cockle due to localized buckling. The results of a finite-element analysis were inconclusive and led Kajanto to the conclusion of local curl as the cause of cockle. Although it may be possible to cause cockles with local curl it can not fully explain the phenomenon of cockle. A simple test can be performed that produces the opposite result anticipated from the mechanism of curl. In this test, a spot of water is placed on a table and a piece of paper is held to the table so that the edges can not curl up on contact with the water. If the paper was free to curl, the edges would curl upwards away from the table. This cannot happen, and the paper remains flat. As the moisture penetrates the sheet, the center of the sheet lifts off the table and produces a cockle with curvature toward the table.

In this test, the movement of the sheet is in contradiction to that predicted by curl, but can easily be explained by local buckling of the sheet. Because the edges of the sheet are constrained, the sheet is not free to expand. This creates compressive stresses in the sheet. When these compressive stresses reach a critical value, the sheet buckles. This argument indicates that local buckling is the key mechanism leading to cockle. Local curl cannot be ignored as a contributing factor to cockle and in some instances may create cockles especially where the paper is completely unrestrained.

A description of the mechanism that leads to cockle is given below.

1. A situation is created such that the expansion and contraction characteristics of the paper varies throughout the plane of the sheet.

2. The paper is in a state such that stresses can be transmitted throughout the sheet.

3. The moisture level of the paper changes so that because of statement 1 some regions shrink or expand more than others.

4. The regions that undergo less shrinkage or more expansion will have compressive stresses.

5. When these compressive stresses in these regions reach a critical value, the sheet buckles locally, thus, producing a cockle.

In all likelihood, imperfections will exist such that instead of a bifurcation buckling to produce a cockle the cockle will steadily grow even for very low compressive stresses. For example, two-sidedness that results in curl would cause out-of-plane displacements even with very low compressive stresses.

Variations in moisture content, coefficients of hygroexpansion, basis weight, degree of beating, anisotropy, and formation are some of the parameters that could lead to nonuniformity in the expansion and contraction of the sheet. This in turn could be caused by variations in stock, stock delivery, and drying methods. A fundamental understanding of cockle treated as a buckling problem could lead to great insight in controlling or eliminating cockle in the paper industry.

ANALYSIS

A hypothesis of the mechanism of cockle based on local buckling of the sheet has been formulated. Evidence from observations pertaining to cockle substantiate this hypothesis. A fundamental analysis of cockle is needed. In addition, refinements to the analysis should produce results that are applicable to practical problems and help in the prediction and control of cockle. If it is assumed that cockle is caused by local buckling of the sheet due to the nonuniform expansion or contraction, then the fundamental problem that predicts buckling due to nonuniform changes in the strain state of the sheet should be able to be formulated with results comparable to the observations of cockle. In the following, an analysis of the local buckling of two concentric plates subjected to moisture changes resulting in nonuniform hygroscopic strains is presented as the fundamental problem capturing the mechanism of cockle.

The most fundamental problem that captures the essence of the formation of a cockle is the local buckling of two concentric plates subjected to changes in moisture. It is assumed that the composite plate is thin and constructed of an inner circular region, denoted region 1 with $0 \le r \le a$, and an outer concentric annular region, denoted region 2 with $a \le r \le b$. It is further assumed that each section is linear elastic, isotropic, and swells and shrinks with changes in moisture levels, but that each section has distinct constant properties as shown in Figure 1. The problem we wish to determine is the in-plane equilibrium of the plate subjected to moisture changes and the critical parameters that lead to buckling of the plate.

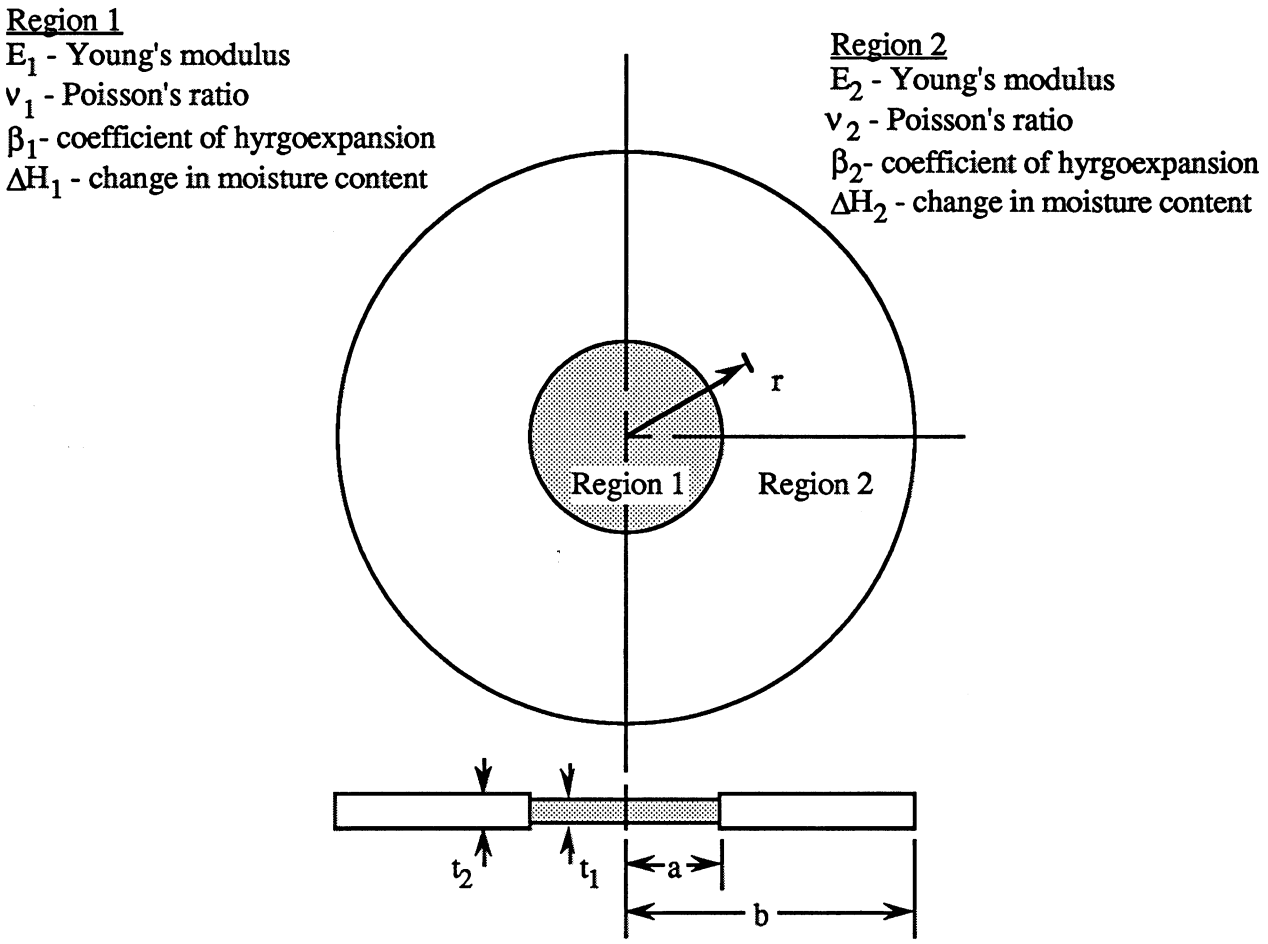

Figure 1. Concentric plates subjected to moisture change.

In-Plane Equilibrium

For the linear elastic and hygroexpansive plate described above, the constitutive equation relating stresses to strains in each section is

$$\begin{Bmatrix} \varepsilon_{ri} \\ \varepsilon_{\theta i} \\ \gamma_{r\theta i} \end{Bmatrix} = \begin{bmatrix} 1/E_i & -\nu_i/E_i & 0 \\ -\nu_i/E_i & 1/E_i & 0 \\ 0 & 0 & 1/G_i \end{bmatrix} \begin{Bmatrix} \sigma_{ri} \\ \sigma_{\theta i} \\ \tau_{r\theta i} \end{Bmatrix} + \begin{Bmatrix} \beta_i \Delta H_i \\ \beta_i \Delta H_i \\ 0 \end{Bmatrix} ; \quad i=1,2 \qquad (1)$$

where in each region, ε_i is the strain tensor; σ_i is the stress tensor; E_i, ν_i, and G_i are elastic constants; β_i is the coefficient of hygroexpansion; and ΔH_i is the change in

moisture content. The subscripts r and θ denote tensor components corresponding to the radial and tangential directions. For example, σ_r is normal radial stress; σ_θ is normal tangential stress; and $\tau_{r\theta}$ is the in-plane shear stress.

The term $\beta_i \Delta H_i$ is the hygroexpansive strain under stress-free expansion of contraction. This could be thought of as the potential strain under unconstrained expansion or contraction. As will be shown below, if the two concentric plates do not have the same potential hygroexpansive strains, the plates will restrict each other, and stresses will exist.

This constitutive equation (1) can be modified to describe anisotropy of the material properties, nonlinear material behavior, or viscoelasticity. Future analyses may require these modifications, but to illustrate the mechanism of cockling, we need only use the constitutive behavior given in equation (1).

The strains are related to the displacements through the kinematic equations. For the present problem, the solution will be symmetric with respect about the radial axis. Therefore, the tangential displacement is zero, and we have in each region

$$\varepsilon_{ri} = \frac{du_i}{dr} \ , \ \varepsilon_{\theta i} = \frac{u_i}{r} \ , \gamma_{r\theta i} = 0 \ ; \ \ i = 1,2 \qquad (2)$$

where u_i is the radial displacement in each region.

The kinematic equations given in equation 2 are valid for infinitesimal strains which are sufficient for the present problem. Other kinematic equations can be used to account for nonsymmetric behavior and finite strains.

Each region of the plate must be in equilibrium. The equations governing equilibrium in both region 1 and region 2 are

$$\frac{d\sigma_{ri}}{dr} + \frac{\sigma_{ri} - \sigma_{\theta i}}{r} = 0 \,, \; \tau_{r\theta i} = 0 \; ; \; i = 1,2. \tag{3}$$

In addition, the two regions of the plate must be in equilibrium with each other and with respect to the conditions prescribed at the edge of the plate. These constraints give rise to the following four boundary conditions:

$$u_1(0) \text{ is finite}, \quad u_1(a) = u_2(a),$$

$$\sigma_{r1}(a)t_1 = \sigma_{r2}(a)t_2, \quad \sigma_{r2}(b) = 0, \tag{4}$$

where t_1 and t_2 are the thicknesses of the plates in regions 1 and 2 respectively. The first two conditions prescribe displacements. Because of the form of equation (3), we expect the solution of the displacement to have a singularity at r=0, and infinite displacement is not physically reasonable. The second displacement condition prescribes that the radial displacement must be continuous across the interface of the two plates.

The second set of boundary conditions in equation (3) prescribes the normal stresses. The first stress condition satisfies the fact that the resultant of the radial stress must be continuous at the interface. The second condition prescribes that the stress at the outer edge is zero reflecting the condition of a free edge. If the edge is restrained, this boundary condition could be changed to either a prescribed restraint force or a prescribed radial displacement.

Equations (1) through (4) constitute a boundary value problem for the radial displacements in each region. The solution for the radial displacements is

$$u_1(r) = r\{\beta_1\Delta H_1 + [\beta_2\Delta H_2 - \beta_1\Delta H_1][1 - (a/b)^2]/\phi\} \qquad 0\le r\le a$$

$$u_2(r) = r\{\beta_2\Delta H_2 - \frac{E_1t_1}{(1-\nu_1)E_2t_2}[\beta_2\Delta H_2 - \beta_1\Delta H_1][(1+\nu_2)\,(a/r)^2 + (1-\nu_2)(a/b)^2]/\phi\} \quad a\le r\le b \quad (5)$$

where $\phi = [1+\frac{(1+\nu_2)E_1t_1}{(1-\nu_1)E_2t_2} + (a/b)^2[\frac{(1-\nu_2)E_1t_1}{(1-\nu_1)E_2t_2} - 1]$.

The stresses in the two regions are

$$\sigma_{r_1}(r) = \sigma_{\theta_1}(r) = \frac{E_1}{(1-\nu_1)}[\beta_2\Delta H_2 - \beta_1\Delta H_1][1 - (a/b)^2]/\phi \qquad 0\le r<a$$

$$\sigma_{r_2}(r) = \frac{E_1t_1}{(1-\nu_1)t_2}[\beta_2\Delta H_2 - \beta_1\Delta H_1][(a/r)^2 - (a/b)^2]/\phi \qquad a<r\le b$$

$$\sigma_{\theta_2}(r) = -\frac{E_1t_1}{(1-\nu_1)t_2}[\beta_2\Delta H_2 - \beta_1\Delta H_1][(a/r)^2 + (a/b)^2]/\phi \qquad a<r\le b. \quad (6)$$

Examination of the equations for the stresses given above shows that if $\beta_1\Delta H_1 = \beta_2\Delta H_2$, then the stresses in the plate are zero. In other words, if the free hygroexpansive strains in each region are equal, then the plate expands/contracts, freely and no stresses are created. On the other hand, if $\beta_1\Delta H_1 \neq \beta_2\Delta H_2$, then one region constricts the expansion/ contraction of the other region resulting in the creation of stresses. It is also of interest to note that the material properties and geometric parameters only affect the magnitude of the stresses and do not influence the existence of the stresses.

Therefore, for the case of an isotropic elastic plate, stresses will exist only if there is a nonuniformity in the free hygroexpansive strains. If the free or potential hygroexpansive

strains are equal, then no stresses will be created. For the case of material anisotropy, stresses would be created if the free hygroexpansive strains in the two regions are different functions of tangential position.

Equations (5) and (6) constitute all the in-plane equilibrium states of the concentric plates for every value of $(\beta_1\Delta H_1 - \beta_2\Delta H_2)$. It is of interest to determine the stability of these states, or for what values of $(\beta_1\Delta H_1 - \beta_2\Delta H_2)$ will the state be unstable. The concentric plates may be unstable if compressive stresses are present in the plate. From the stress results given in equation (6), the following can be concluded about the stresses in each region:

If $\beta_2\Delta H_2 > \beta_1\Delta H_1$,

then $\sigma_{r_1}(r)$, $\sigma_{\theta_1}(r)$, and $\sigma_{r_2}(r)$ are tensile, and $\sigma_{\theta_2}(r)$ is compressive.

and

If $\beta_2\Delta H_2 < \beta_1\Delta H_1$,

then $\sigma_{r_1}(r)$, $\sigma_{\theta_1}(r)$, and $\sigma_{r_2}(r)$ are compressive, and $\sigma_{\theta_2}(r)$ is tensile.

This implies that during expansion ($\beta\Delta H > 0$) compressive stresses will exist in the region that would expand the most under free expansion. During contraction ($\beta\Delta H < 0$), compressive stresses will exist in the region that would undergo the least shrinkage in free contraction. Under these circumstances, local buckling of the regions various regions could be expected.

Local Buckling of the Plate

Local buckling of the plate may occur when the magnitude of the compressive stresses in a region exceeds the critical buckling load of that region. For example, assume that local buckling may occur in the inner region which would correspond to $\beta_1\Delta H_1 > \beta_2\Delta H_2$. For

this case both the radial and the tangential normal stresses are compressive. The critical buckling load in this region is determined from the following differential equation for the out-of-plane displacement, w, and four appropriate homogeneous boundary conditions.

$$\frac{d^4w}{dr^4} + \frac{2d^3w}{r\,dr^3} - \frac{1}{r^2}\frac{d^2w}{dr^2} + \frac{1}{r^3}\frac{dw}{dr} + \lambda\left[\frac{d^2w}{dr^2} + \frac{1}{r}\frac{dw}{dr}\right] = 0 \quad 0 \le r \le a \qquad (7)$$

where $\lambda = 12[\beta_1\Delta H_1 - \beta_2\Delta H_2][1-(a/b)^2][1+\nu_1]/(t_1^2\phi)$. The solution of this eigenvalue problem will yield the critical buckling load, or in this case, a critical value of $(\beta_1\Delta H_1 - \beta_2\Delta H_2)$. For the present problem, this would give

$$[\beta_1\Delta H_1 - \beta_2\Delta H_2]_{cr} = Ct_1^2\phi/\{[1-(a/b)^2][1+\nu_1]\} \qquad (8)$$

where C is a known constant corresponding to the lowest eigenvalue. Therefore, we find that the inner region of the plate will buckle only if the differences in the potential free hygroexpansive strains of each plate reach a critical value.

Study of equation (8) reveals the following conclusions about the local buckling in the inner region of the concentric plates.

- Under conditions of swelling, buckling may occur in the inner region only if the free hygroexpansive strain in the inner region is larger than that of the outer region.

- Under conditions of shrinkage, buckling may occur in the inner region only if the free hygroexpansive strain in the inner region is smaller than that in the outer region.

- The nonuniformity in free hygroexpansive strains is due only to differences in coefficients of hygroexpansion or differences in moisture content.

- The critical difference in hygroexpansive strains will decrease as the square of the thickness of the inner plate decreases.

- The magnitude of the critical difference in hygroexpansive strains will depend on the ratio of Young's moduli time the thickness (Et) in the two regions and the Poisson's ratios (ν).

- The magnitude of the differences in hygroexpansive strains will depend on the ratio of the radii of the two plates (a/b).

Note the details of this analysis need to be worked out, and the case of local buckling in the outer region needs to be addressed.

DISCUSSION

When the preliminary results of the fundamental analysis are compared to the laboratory results of Brecht [21], the mechanism of local buckling due to nonuniformities in the hygroexpansive characteristics of the sheet appears to be a reasonable explanation for cockle. Brecht [21] found that upon drying, regions that were initially drier always formed cockles. These initially drier regions have less potential shrinkage than the initially wetter sections. Upon drying these sheets, the wetter sections compress the drier regions and cockle results. This is analogous to the analytic result that the inner section would buckle if the potential shrinkage in the inner section is less than the potential shrinkage in the outer section.

For Brecht's samples, cockles were observed in initially drier inner circular regions. This observation is in agreement with the analysis that showed that the inner region could

buckle under the analogous conditions. When the outer regions in Brecht's samples were drier, he observed a star-like buckled pattern in the outer region. The axes of these buckles were aligned close to lines that were perpendicular to the circumference of the inner region. The stress analysis given above revealed that for the case of the outer region having less potential shrinkage, the only compressive stress was the tangential normal stress in the outer region. Therefore, it is expected that an analysis of local buckling in the outer region will yield a similar star pattern. In fact, a very similar analysis of the flange wrinkling of deep-drawn sheet metals does predict this type of buckled pattern [24].

The analysis showed that variations in material properties and geometric parameters effect the magnitude of the stresses, but only contribute to cockling if accompanied with a nonuniformity in the free hygroexpansive strains. This is in agreement with the observations made in the literature [2,4] that cockles were related to changes in basis weight because these nonuniformities in basis weight affected the uniformity of drying rates.

It is of interest to note that in the above analysis cockle was predicted on the basis of local buckling only, and not local curl. Therefore, one can expect that many cockle problems may be the result of local buckling. Under certain circumstances, cockle may result from local curl. In fact, the results of this program may show that some types of cockle are due to local buckling and other types are a result of local curl. This issue remains to be addressed.

The analysis presented above is linear elastic, and upon reversal of the moisture changes, the buckling would disappear. This is not an observed characteristic of cockle in paper. A paper that is originally flat, then wetted to produce cockles, then redried, will not return

to a flat state. This implies that nonlinear material models are needed to improve the analysis of cockle in paper. In addition, the properties of paper are known to be anisotropic, and this can be seen in the cockle of some papers which have a preferred orientation. Therefore, anisotropy of material properties must be added to the model. With the expected complexities of such a model, numerical methods will be employed for the development of future analyses. Finite-element methods will provide a useful tool for the prediction and study of cockle in paper.

REFERENCES

1. Lavigne, J. R., Pulp and Paper Dictionary, Revised Edition, Technical editor K. L. Patrick, Miller Freeman Books, San Francisco, CA, 1993.

2. Smith, S. F., "Dried-in Strains in Paper Sheets and Their Relation to Curling, Cockling, and Other Phenomena," *The Paper-Maker and British Paper Trade Journal*, Vol. 110, No. 3, March 1950, pp. 185-192.

3. "Wrinkles and Cockles," *Paper Trade Journal*, Vol. 53, No. 19, November 9, 1911, pp. 60. (unauthored)

4. Dittmann, R., "The Influence of Hydraulic Pulsations on Cockles," 1992 Practical Aspects of Pressing and Drying Short Course, TAPPI Press, 1992, pp. 237-240.

5. Stamm, F. C., "The Effect of Improper Drying on Quality," *Paper Mill News,* Vol. 64, No. 25, June 21, 1941, pp. 124, 126.

6. Van Patten, M. D., "Functions of a Dryer Felt," *Paper Mill News*, Vol. 78, No. 24, June 25, 1955, pp. 118-128.

7. Moore, B., "Take a Second Look at Bottom Felts!," *PIMA*, Vol. 78, No. 1, January 1989, pp. 29-31.

8. Wedel, G., "Drying Restraint in a Single-Tier Dryer Section," *TAPPI Proceedings of 1989 Annual Meeting*, New York, NY, March 12-15, 1989, pp. 23-29.

9. Wedel, G., "Drying Restraint Helps Improve Sheet Edge Quality," *PIMA*, Vol. 71, No. 11, November 1989, pp. 27-29.

10. Chance, J. L., "Restrained Drying: Commercial Experience," *Appita*, Vol. 45, No. 2, March 1992, pp. 131-133.

11. Reese, J. R., "Observations from Testing Dryer Section Performance," *TAPPI Proceedings of the 1992 Engineering Conference*, Boston, MA, September 14-17, 1992, pp. 629-637.

12. Bell, N. E., "Remoisturizing in the Dryer Section," *TAPPI Proceedings of the 1986 Engineering Conference*, Atlanta, GA, September 22-25, 1986, pp. 315-317.

13. Cunnington, R., Kelly, D., and McIvor, A., "Press Rebuild, Refiner Replacement," *Pulp and Paper*, Vol. 54, No. 9, September 1980, pp. 110-114.

14. "Hard Cockles in Loft Dried Paper," TAPPI Special Inquiry No. 145, January 1930.

15. Cooper, E. W. G., " The Cause of Grainy Edges, Curl, and Cockles in Paper," *TAPPI Journal*, Vol. 20, 1937, pp. 173-179.

16. Chodhury, S. C., "Cockling in Paper and Board," *IPPTA*, Vol. 4, No. 3, October, 1967, pp. T101-T102.

17. Gallay, W., "Stability of Dimensions and Form of Paper," *TAPPI Journal*, Vol. 56, No. 12, December 1973, pp. 90-95.

18. Uesaka, T., " Dimensional Stability of Paper: Upgrading Paper Performance in End Use," *Journal of Pulp and Paper Science*, Vol. 17, No. 2, March 1991, pp. J39-J46.

19. Gooray, A. and Agbezuge, L., "Paper Deformation Due to Ink Jet Printing," October 1992, pp. 312-317.

20. Kajanto, I. M., "Finite Element Analysis of Paper Cockling," Products of Paper Making, Transactions of the Tenth Fundamental Research Symposium, Vol. 1, Edited by C. F. Baker, Oxford, Septtember 1993, pp. 237-262.

21. Brecht, W., "Beating and Hygrostability of Paper," Fundamentals of PaperMaking Fibers, Transactions of the Symposium Held at Cambridge, September 1957, Edited by F. Bolam, pp. 241-262.

22. Shriver, E. H., "A Fundamental Program of Research on Cockle in Paper," Problem Number 2 - Set B, Third Year Program, The Institute of Paper Chemistry, December 4, 1947.

23. Brecht W., Müller, F., Weiss, H., " Uber das Blasigwerden von Papieren," *Das Papier*, Vol. 9, No. 7/8, April 1955, pp. 133-142.

24. Yu, T. X. and Johnson, W., "The Buckling of Annular Plates in Relation to the Deep-Drawing Process," *International Journal of Mechanical Sciences*, Vol. 24, No. 3, 1982, pp. 175-188.